Macromitrium Brid. (Bryophyta, Orthotrichaceae) in Brazil: a molecular approach

Daiane Valente Valente · Denilson Fernandes Peralta · Michael Stech · Paulo Eduardo Aguiar Saraiva Câmara

DOI:
https://doi.org/10.1007/s40415-023-00935-3

Brazilian Journal of Botany (2023) 46:925–946
https://doi.org/10.1007/s40415-023-00935-3

SYSTEMATICS & PHYLOGENY - ORIGINAL ARTICLE

Macromitrium Brid. (Bryophyta, Orthotrichaceae) in Brazil: a molecular approach

Daiane Valente Valente[1] · Denilson Fernandes Peralta[2] · Michael Stech[3,4] · Paulo Eduardo Aguiar Saraiva Câmara[1]

Received: 7 January 2023 / Revised: 8 August 2023 / Accepted: 5 September 2023 / Published online: 23 September 2023

Abstract

The Brazilian species of *Macromitrium* Brid. presents many taxonomic and systematic problems, mainly because the morphological characters used for species identification were not well established in the past, and many species have no phylogenetic position established yet. In this paper, we aim (i) to test the monophyly of *Macromitrium* based on the phylogenetic analysis of Brazilian species using four markers from different genomic compartments (*trn*L-F, *rps*4, *nad*5 and 26S), (ii) if not a monophyletic group, to delimit which Brazilian species belong to true *Macromitrium* and, (iii) to test the potential of *trn*G-R, *trn*L-F, and ITS markers to resolve the phylogenetic relationships and species delimitations within *Macromitrium*. Our data demonstrate that *Macromitrium* is not monophyletic, but split into three different groups: MG1 (true *Macromitrium*), MG2 (new genus *Pseudomacromitrium*), and MG3 (the monospecific new genus *Aureomacromitrium*). Our barcoding data suggest that the best candidate marker for DNA barcoding was *trn*G-R due to its easy amplification and ability to discriminate all the analyzed species. The nuclear marker ITS was easy to amplify and more variable than the plastid markers, but alignment difficulties and more frequent fungal contaminations are potential drawbacks. *Trn*L-F had a low discrimination potential. Our results provide important data on the phylogeny of the Macromitrioideae, serving as a basis for the expansion of the phylogenetic studies for the other *Macromitrium* species that occur in the world, as well as providing a new tool to solve the current problems of identification of Brazilian species.

Keywords DNA barcoding · Phylogeny · Moss · Molecular markers · Macromitrioideae

1 Introduction

The cosmopolitan moss family Orthotrichaceae Arn. comprises more than 800 species in approximately 20 genera, divided into two subfamilies, the acrocarpous Orthotrichoideae and the cladocarpous Macromitrioideae (Goffinet and Vitt 1998; Frey and Stech 2009). *Macromitrium* Brid. is the third largest moss genus in the world, with an estimated 365, mostly tropical and subtropical, species (Crosby et al. 1999; Frey and Stech 2009), of which roughly one-third (128) have been thoroughly treated in revisions (Crosby et al. 1999). The number of little known taxa has decreased due to the accomplishment of taxonomic treatments and floras for Japan (Noguchi 1967), New Zealand and Australia (Vitt and Ramsay 1983, 1985a,b, 1986), southern and eastern Africa (Rooy and Wijk 1992; Wilbraham 2015, 2016), Papua New Guinea (Vitt et al. 1995), New Caledonia (Thouvenot 2019), China (Guo et al. 2012), Mexico (Sharp et al. 1994), and Central America (Allen 2002).

However, insufficient morphological and taxonomic knowledge, superfluous names, and the absence of good keys still hamper the identification of *Macromitrium* species in several geographic regions, such as Africa (Wilbraham 2016), South America, and the Pacific (Yu et al. 2018). In addition, the morphological characters used for species identification are not well established with many overlaps (Allen 2002). There are 54 *Macromitrium* species recorded

✉ Denilson Fernandes Peralta
denilsonfperalta@gmail.com

[1] Laboratório de Criptógamas, Departamento de Botânica, Universidade de Brasília (UnB), Campus Universitário Darcy Ribeiro, Brasília, DF, Brazil

[2] Instituto de Pesquisas Ambientais, Av. Miguel Stéfano, 3687, São Paulo, SP CEP04301-012, Brazil

[3] Naturalis Biodiversity Center, P.O. Box 9517, 2300 RA Leiden, The Netherlands

[4] Leiden University, Leiden, The Netherlands

in Brazil, but 34 were considered poorly known by Costa et al. (2011). Of the remaining 20 species (including six species endemic to Brazil) listed in the current Brazilian Online Flora (http://floradobrasil.jbrj.gov.br/), still 50% are known only by the types and/or very ancient collections according to *SpeciesLink* (http://splink.cria.org.br/).

One hypothesis for the taxonomic complexity and problems with interpreting morphological character variation is that *Macromitrium* may not be monophyletic (Goffinet et al. 1998; Frey and Stech 2009). However, the molecular studies involving genera of Orthotrichaceae published to date either do not include species of *Macromitrium* (Cox et al. 2010; Goffinet and Buck 2004) or their taxon sampling is insufficient to test this hypothesis (Goffinet et al. 1998; Li et al. 2013). Phylogenetic studies of extended molecular datasets are necessary for a better understanding of the circumscription of *Macromitrium*.

In addition, DNA barcoding (Hebert et al. 2003) should be implemented as a molecular tool to distinguish *Macromitrium* species and to infer the diagnostic value of morphological characters for species identification. DNA barcoding of plants is generally performed based on a combination of two or more genetic loci. Most existing studies on bryophytes have compared the highly variable nuclear ribosomal ITS regions and various markers from the chloroplast genome (overview in Valente et al. 2019). In the Orthotrichaceae, Li et al. (2013) tested the use of the chloroplast markers *trn*G and *trn*L-F for Chinese *Macromitrium* species, while Valente et al. (2019) tackled species delimitations in Brazilian *Schlotheimia* Brid. based on *trn*L-F, *trn*G-R and ITS sequence data.

The present study employs an extended molecular dataset (four markers from all three genomic compartments) to study the evolution and delimitation of *Macromitrium* in Brazil. Specifically, we aim to (i) to test whether Brazilian species of *Macromitrium* form a monophyletic group, (ii) if not a monophyletic group, to delimit if (and which) Brazilian species belong in true *Macromitrium*, and (iii) test the potential of *trn*G-R, *trn*L-F, and ITS markers for molecular identification of the Brazilian *Macromitrium* species.

2 Materials and methods

Taxon and molecular marker sampling – Phylogenetic analyses to test the monophyly of *Macromitrium* followed the sampling of Cox et al. (2010). Albeit not including *Macromitrium*, Cox et al. (2010) employed sequences from three markers, nuclear ribosomal 26S, mitochondrial *nad*5, and chloroplast *rps*4, from most other genera of Macromitrioideae. To those we added chloroplast *trn*L-F sequences of the same taxa that were available on GenBank from other studies, and own sequences from all four markers. The resulting dataset 1 included sequences of eight genera of the Macromitrioideae [*Bryomaltaea* Goffinet, *Cardotiella* Vitt, *Desmotheca* Lindb., *Groutiella* Steere, *Leiomitrium* Mitt., *Macrocoma* (Hornsch. ex Müll.Hal.) Grout, *Matteria* Goffinet and *Schlotheimia*] from GenBank as well as new sequences (six species of *Macromitrium*, one of *Macrocoma*, and one of *Groutiella)* from Brazil. In addition, we carried out a separate analysis based on all *trn*L-F sequences available (Genbank and own data), including the type species of *Macromitrium*, *M. pallidum* (P. Beauv.) Wijk & Margad. This dataset 2 aimed to delimit which Brazilian species, if any, belonged to true *Macromitrium*, and comprised 14 species of *Macromitrium* and 11 species of eight other genera of the subfamily Macromitrioideae. Two species of different genera of subfamily Orthotrichoideae were used as outgroup representatives following Goffinet et al. (1998). Voucher information and Genbank accession numbers are listed in Appendix S1.

For molecular species discrimination of Brazilian *Macromitrium*, we focused on the three DNA regions (chloroplast *trn*L-F and *trn*G-R as well as nuclear ribosomal ITS) that were previously tested for *Schlotheimia* in Brazil (Valente et al. 2019). The three potential DNA barcoding markers comprise two non-coding parts each (*trn*L-F: *trn*L group I intron and *trn*L-*trn*F intergenic spacer, *trn*G-R: *trn*G group II intron and *trn*G-*trn*R intergenic spacer, ITS: internal transcribed spacers ITS1 and ITS2).

After the study of type material of *Macromitrium* species from herbaria BM, E, G, GOET, L, NY, PACA, PC, SP, R, and RB, by the first author, we considered several names currently accepted for Brazil (http://floradobrasil.jbrj.gov.br/) to be synonymous (pers.obs.) of older names. Based on morphology we recognized 10 putative species, which are included here to test whether molecular data support the morphological species concept. Depending on availability and sequencing success, we used 2–4 individuals for each putative species, sampled from herbarium collections or from fresh samples collected in the field. Voucher information and Genbank accession numbers are listed in Appendix S2. Since sequences of taxa of subfamily Orthotrichaceae were difficult to align with*Schlotheimia*, especially for the highly variable marker ITS, we used *Macromitrium catharinense* Paris as outgroup based on the maximum support of the topology in all analyses of the present phylogenetic reconstructions.

DNA extraction, amplification and sequencing – DNA extraction and PCR amplification (Mullis and Faloona 1987) were performed at the Molecular Biology of Plants lab, Botany Department, University of Brasília. Total genomic DNA was extracted using the mini-CTAB protocol (Doyle and Doyle 1987), with modifications (Câmara 2010). The PCR amplification mixture had a total volume of 50 µl and

contained 5 µl of 5 × thermophilic buffer, 5 µl of 50 mM $MgCl_2$, 0.5 µl *Taq* polymerase (Promega, Madison, Wisconsin, U.S.A.), 2 µl of BSA (10 mg/ml), 4 µl of 1 mM dNTP, 2.5 µl of each primer (10 µM), 2.0 µl of DNA and 26.5 µl of water. Primer information for all molecular markers is shown in Table 1. The PCR profile for all markers was 95 °C (30 s), 48 °C–56 °C (45 s), 72 °C (1 min) for 35 cycles, always preceded by an initial melting step of 1 min at 95 °C and with a final extension of 72 °C for 5 min. PCR products were purified and sequenced by Macrogen (Seoul, South Korea).

Phylogenetic and species delimitation analysis – Sequences were assembled and edited using Geneious v.6.1.6 (Biomatters 2010), initially aligned using ClustalX 2.1 (Larkin et al. 2007), then manually adjusted using PhyDE v.0.9971 (Müller et al. 2006) and exported as NEXUS files. Phylogenetic analyses of the Macromitrioideae were done under maximum parsimony (MP), maximum likelihood (ML) and Bayesian inference (BI), for each marker separately (26S, *nad*5, *rps*4, *trn*L-F) as well as for combined matrices of 26S, *nad*5, and *rps*4 (as in Cox et al. 2010).

To discriminate Brazilian *Macromitrium* species, we followed a step-wise approach. Firstly, putative species were inferred from tree-based analyses [neighbor-joining (NJ; Saitou and Nei 1987), MP, ML, BI], based on topological congruence between markers (*trn*L-F, *trn*G-R, ITS) and clade support. Analyses were carried out for each marker separately as well as for all combinations of two markers, and all three markers combined. Secondly, an automated species delimitation approach, Automatic Barcode Gap Discovery (ABGD; Puillandre et al. 2012), which uses a pairwise genetic distance-based method to find non-overlapping intra- and interspecific genetic distance distributions within the sequence dataset, was employed as an alternative to construct hypothetical candidate species from the molecular data.

Maximum parsimony and NJ analyses were performed in PAUP* v.4.0b10 (Swofford 2002). Heuristic searches under MP were performed with 1000 random addition replicates and tree-bisection-reconnection (TBR) branch swapping, saving a maximum of 10,000 trees. All characters were unordered and equally weighted, and gaps were either treated as missing data or coded as informative by Simple Indel Coding (SIC; Simmons and Ochoterena 2000) as implemented in SeqState (Müller 2005). Neighbor-joining analyses were performed using the "Kimura 2-parameter" (K2P) model (Kimura 1980). Besides, intraspecific and interspecific variation was inferred from the pairwise distances, calculated using the K2P model in MEGA7 (Kumar et al. 2015).

For ML and BI analyses, the best-fit model of evolution for each locus was obtained based on the Akaike information criteria using jModeltest 3.06 (Posada 2008). ML analyses were carried out using RAxML v7.2.6 (Silvestro and Michalak 2012). Clade support for MP and ML was assessed from bootstrap analyses with 1000 replicates (Felsenstein 1985).

Bayesian inference analyses were carried out in MrBayes v. 3.2.6 (Ronquist et al. 2012). Two runs with four Markov Chain Monte Carlo chains each were run for 5,000,000 generations. Chains were sampled every 1000 generations and the respective trees were written to a tree file. Convergence of runs was verified by ensuring that the average standard deviation of split frequencies was < 0.01. Tracer 1.5 (Rambaut and Drummond 2013) was used to determine when the tree sampling stabilized. The first 25% of the trees were discarded as 'burn-in.' A majority rule consensus tree and posterior probabilities were calculated from the resulting trees.

For species discrimination and phylogenetic analyses we follow Valente et al. (2019) where were considered supported as posterior probability [PP] only ≥ 0.95

Table 1 *Primers used* for amplification in phylogenetic and DNA barcoding analyses

Primers	Region	Direction	Sequence 5'-3'	Annealing temp. °C	Reference
18F	ITS (nuclear)	Forward	GGA AAG AGA AGT CGT AAC AAG G	48°	Stech and Frahm (1999)
25R	ITS (nuclear)	Reverse	TCC TCC GCT TAG TGA TAT GC	48°	Stech and Frahm (1999)
B	*trn*G-R (Chloroplast)	Forward	GCG GGT ATA GTT TAG TGG	53°	Pacak et al. (2000)
Cm	*trn*L-F (Chloroplast)	Forward	CGA AAT TGG TAG ACG CTG CG	56°	Stech et al. (1999)
Fm	*trn*L-F (Chloroplast)	Reverse	ATT TGA ACT GGT GAC ACG AG	56°	Stech et al. (1999)
LS0F	26S (nuclear)	Forward	ACC CGC TGT TTA AGC ATA T	48°	Shaw (2000)[a]
*nad*5F4	*nad*5 (mitochondrial)	Forward	GAA GGA GTA GGT CTC GCT TCA	53°	Shaw et al. (2003)
*nad*5R3	*nad*5 (mitochondrial)	Reverse	AAA ACG CCT GCT GTT ACC AT	53°	Shaw et al. (2003)
Rps5	*rps*4 (Chloroplast)	Forward	ATG TCC CGT TAT CGA GGA CCT	52°	Nadot et al. (1994)
*trn*as	*rps*4 (Chloroplast)	Reverse	TAC CGA GGG TTC GAA TC	52°	Souza-Chies et al. (1997)
TRNR22R	*trn*G-R (Chloroplast)	Reverse	CTA TCC ATT AGA CGA TGG ACG	53°	Nagalingum et al. 2007
zLS12R	26S (nuclear)	Reverse	ATC GCC AGT TCT GCT TAC CA	48°	Shaw (2000)

and to bootstrap support [BS] high (≥ 95%), moderate (85 − ≤ 94%), and lower (≤ 84%). The values of BS are presented in results as (minimum/maximum).

Automatic Barcode Gap Discovery analyses were carried out on the online web server (http://wwwabi.snv.jussieu.fr/public/abgd/abgdweb.html). The dataset of three markers combined (*trn*L-F + *trn*G-R + ITS) was used with the input file in fasta format, and the Kimura-2-parameter model and a range of different settings employed. Since the latter resulted in the same number of initial partitions, the final parameters were set as follows: Pmin = 0.001, Pmax = 0.01, Steps = 50, X = 1.1, Nb bins = 100.

3 Results

Phylogenetic analysis – Alignment statistics, best-fitting models of evolution, and tree scores are summarized in Table 2. Trees based on analysis of individual markers and on different analysis methods differed only in degree of resolution but did not show statistically supported conflicting topologies, indicating that the markers of dataset 1 could be combined.

Phylogenetic analysis of dataset 1 (Fig. 1) reveals that the Brazilian *Macromitrium* species do not form a monophyletic group, but are split into three different clades, here named *Macromitrium* group (MG) 1, MG2, and MG3, respectively. Clade MG1 was not supported in MP, but received moderate bootstrap support in ML (88%) and a posterior probability of 1 in BI. This clade was composed of the species *Macromitrium richardii* Schwägr. and *M. microstomum* (Hook. & Grev.) Schwägr. and was resolved as sister to *Desmotheca* Lindb., with high support in ML (97% BS) and a PP of 1 in BI. Clade MG2 received high support in ML (BS 96%) and BI (PP 1). It contained the species *Macromitrium levatum* Mitt., *M. guatemalense* Müll.Hal., *Macromitrium punctatum* (Hook. & Grev.) Brid. and *M. argutum* Hampe, and was resolved as sister to *Groutiella* Steere, with equally high support in ML and BI. Clade MG3, formed by the single species *Macromitrium catharinense* Paris, sister group relationship to the MG2-*Groutiella* clade, received lower support (77% BS) in ML and a PP of 1 in BI.

The analyses of dataset 2 (Fig. 2), based on *trn*L-F alone, corroborated the results of dataset 1 in terms of the splitting of the Brazilian *Macromitrium* species in three clades. In addition, they proved that clade MG1 corresponds to *Macromitrium* s.str., since it included the type species *M. pallidum*. Apart from the Brazilian *M. richardii* and *M. microstomum* and the African *M. pallidum*, all additionally included Asian species (*M. gymnostomum* Sull. & Lesq., *M. taiheizanense* Nog., *M. cavaleriei* Cardot & Thér., *M. japonicum* Dozy & Molk., *M. rhacomitrioides* Nog., and *M. incurvifolium* (Hook. & Grev.) Schwägr.) fell into clade MG1 as well.

Molecular species discrimination (DNA barcoding) – PCR amplification and sequencing success using a single primer pair was high for all three markers. The amplification potential of the *trn*G-R region was 93%, followed by *trn*L-F and ITS (both 89%). All sequences were of good quality, with 41 *trn*G-R, 39 *trn*L-F and 39 ITS sequences included in the analyses.

Characteristics of sequence lengths and variability of all three markers are summarized in Tables 3 (clade MG1) and 4 (clade MG2), respectively. Relative to the plastid markers trnG-R and trnL-F, the nuclear ITS marker was larger (36/67% in MG1, 46/70% in MG2, respectively) and more variable (64/99% in MG1, 62/82% in MG2, respectively) than the plastid markers *trn*G-R and *trn*L-F. Sequences were more variable in MG2, presenting 2.6% more informative sites in ITS, 2.7% in *trn*G-R, and 5.6% in *trn*L-F than in MG1.

Phylogenetic trees of each individual marker (*trn*L-F, *trn*G-R and ITS) did not show incongruence in terms of

Table 2 Alignment statistics, best-fitting models of evolution, and tree scores for the phylogenetic datasets 1 and 2

DNA Region	*trn*L-F	*rps*4	*nad*5	26S	Combined	*trn*L-F
Dataset	1	1	1	1	1	2
Taxa included	25	33	25	19	32	37
Variable sites	135	186	158	118	594	160
Parsimony informative sites	75	100	91	56	321	82
Number of trees retained	36	1200	2760	72	9	1560
Number of best trees	181	255	180	182	816	222
Tree	193	280	203	212	844	232
CI	0.777	0.721	0.798	0.646	0.763	0.776
RI	0.794	0.760	0.747	0.522	0.764	0.835
Model	TIM1 + I + G	TVM + G	TPM3uf + G	TIM2 + I + G	TVM + I + G	TrN + G
Log Likelihood	− 1350.1358	− 2053.5605	− 3390.1241	− 2157.4561	− 9469.3062	− 1566.0043

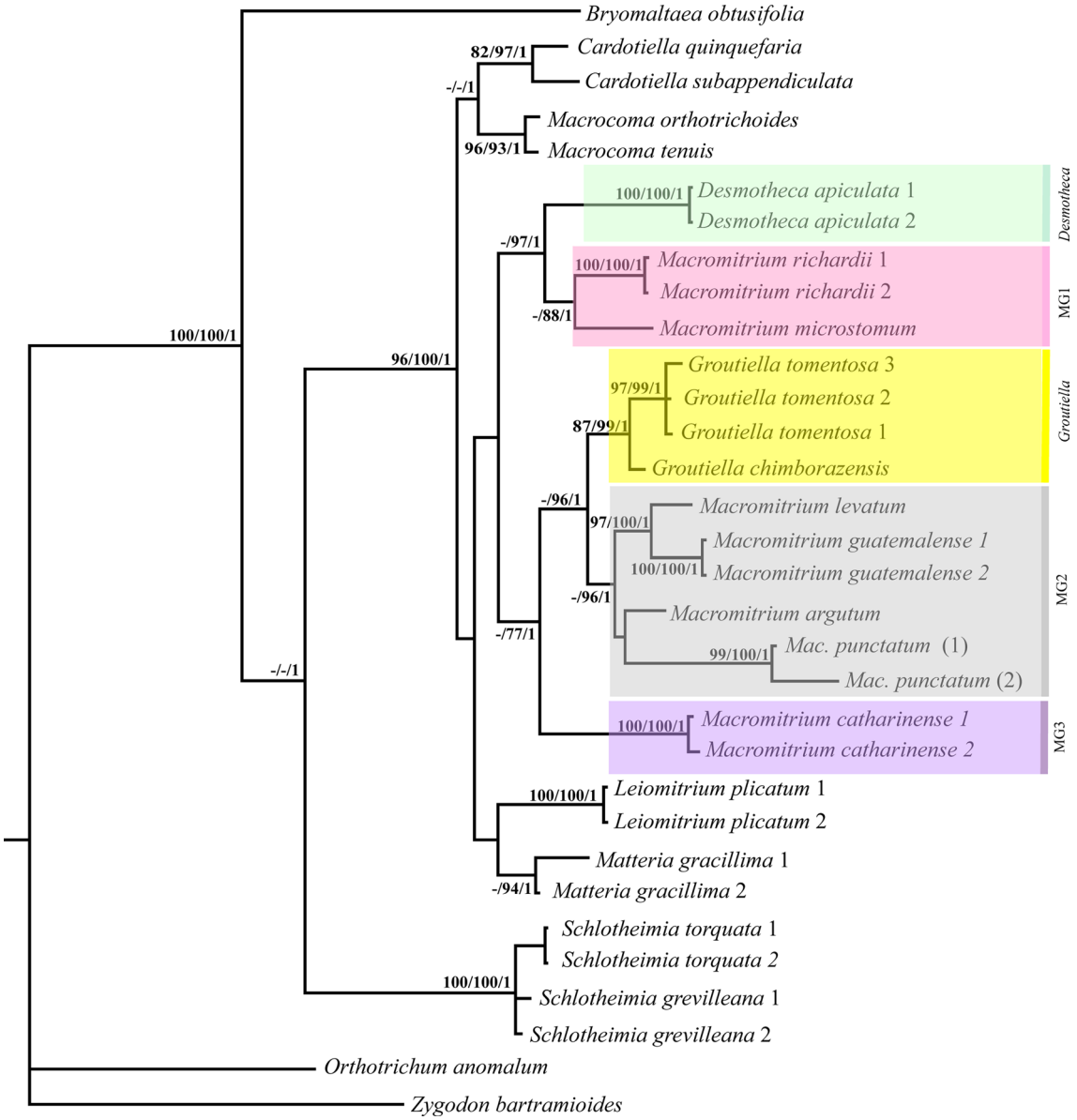

Fig. 1 Phylogram obtained from Bayesian inference (BI) based on combined *trn*L-F + *rps*4 + *nad*5 + 26S sequences of 32 specimens of Orthotrichaceae, including indels coded by simple indel coding. Bootstrap support for Maximum Parsimony (MP), Maximum Likelihood (ML) and Bayesian posterior probabilities is shown, respectively, in each clade and node. MG1: *Macromitrium* group 1; MG2: *Macromitrium* group 2; MG3: *Macromitrium* group 3

well-supported branches (data not shown), indicating that the markers could be combined. The Bayesian inference tree based on the maximum amount of information (three markers combined with indels coded by SIC) is shown in Figs. 3 and 4 for MG1 and MG2, respectively, together with a summary of the results obtained from all phylogenetic and species delimitation methods used.

The ITS marker alone as well as the combinations *trn*L-F + *trn*G-R, *trn*L-F + ITS, *trn*G-R + ITS, and all markers combined, were efficient to discriminate 100% of the putative species clades for both groups (MG1: clades A/B in Fig. 3; MG2: clades A – G in Fig. 4), with moderate support (*M. microstomum* clade, ML analysis, ITS and *trn*L-F + ITS markers; *M. longifolium* clade, NJ analysis, *trn*L-F + *trn*G-R) or high support in all analyses (Tables 5 and 6). The *trn*G-R marker alone showed good performance in ML and BI analyses, with high support and 100% discrimination potential of MG2 species, whereas the NJ and MP analysis of *trn*G-R discriminated only 72% of the species with high support. For MG1, this marker separated both species with maximum support in all analyses. The *trn*L-F marker performed least for both MG1 and MG2. For MG2, percentages

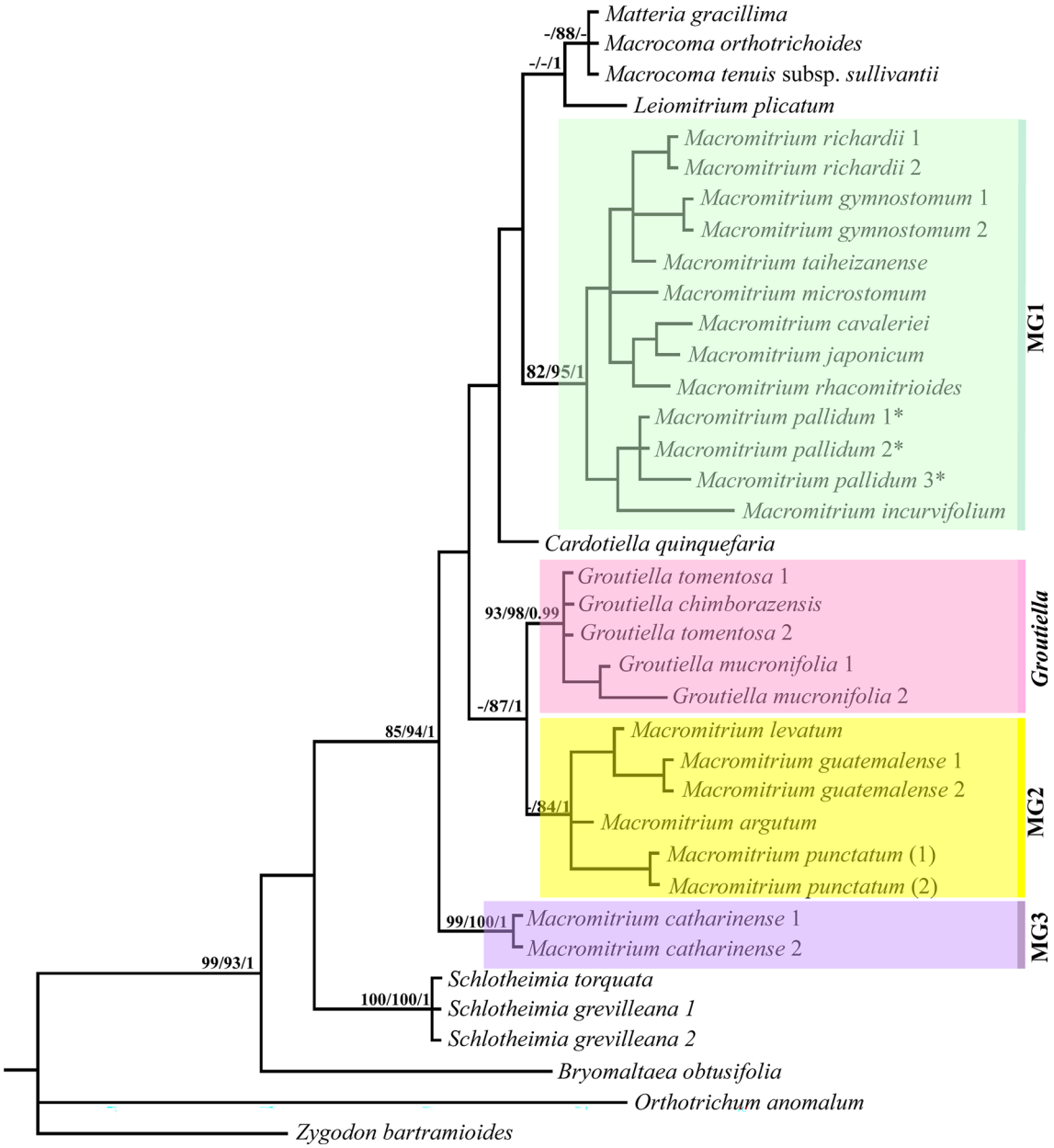

Fig. 2 Phylogram obtained from Bayesian inference (BI) based on *trn*L-F marker sequences of 38 specimens of Orthotrichaceae, including indels coded by simple indel coding. Bootstrap support for Maximum Parsimony (MP), Maximum Likelihood (ML) and Bayesian posterior probabilities is shown in each clade and node. MG1: *Macromitrium* group 1; MG2: *Macromitrium* group 2; MG3: *Macromitrium* group 3. (*) type species

Table 3 *Macromitrium* (Group 1)

Marker	Fragment length (nt)	Alignment length with outgroup	Alignment length without outgroup	Conserved sites (%)	Variable sites (%)	Parsimony informative sites (%)	Number Indels	Parsimony informative indels	Medium pairwise distance
*trn*L-F	390 – 403	407	390	386(99)	4(1)	4(1)	0	0	0.006
*trn*G-R	739 – 744	753	752	725(96,4)	27(3,6)	27(3,6)	6	4	0.020
ITS	898 – 947	1474	1163	1063(91,4)	100(8,6)	75(6,5)	78	68	0.062

Characterization of each marker. The data for conserved sites, variable sites, parsimony informative sites, parsimony informative indels and medium pairwise distances refer to the matrix without outgroup

Table 4 *Macromitrium* (Group 2)

Marker	Fragment length (nt)	Alignment length with outgroup	Alignment length without outgroup	Conserved sites (%)	Variable sites (%)	Parsimony informative sites (%)	Number Indels	Parsimony informative indels	Medium pairwise distance
*trn*L-F	403 – 412	413	412	388 (94,2)	24 (5,8)	23 (5,6)	3	2	0.013
*trn*G-R	734 – 744	747	747	698 (93,4)	49 (6,6)	47 (6,3)	11	8	0.019
ITS	678 – 898	1681	1379	1211 (87,8)	168 (12,2)	125 (9,1)	265	196	0.064

Characterization of each marker. The data for conserved sites, variable sites, parsimony informative sites, parsimony informative indels and medium pairwise distances refer to the matrix without outgroup

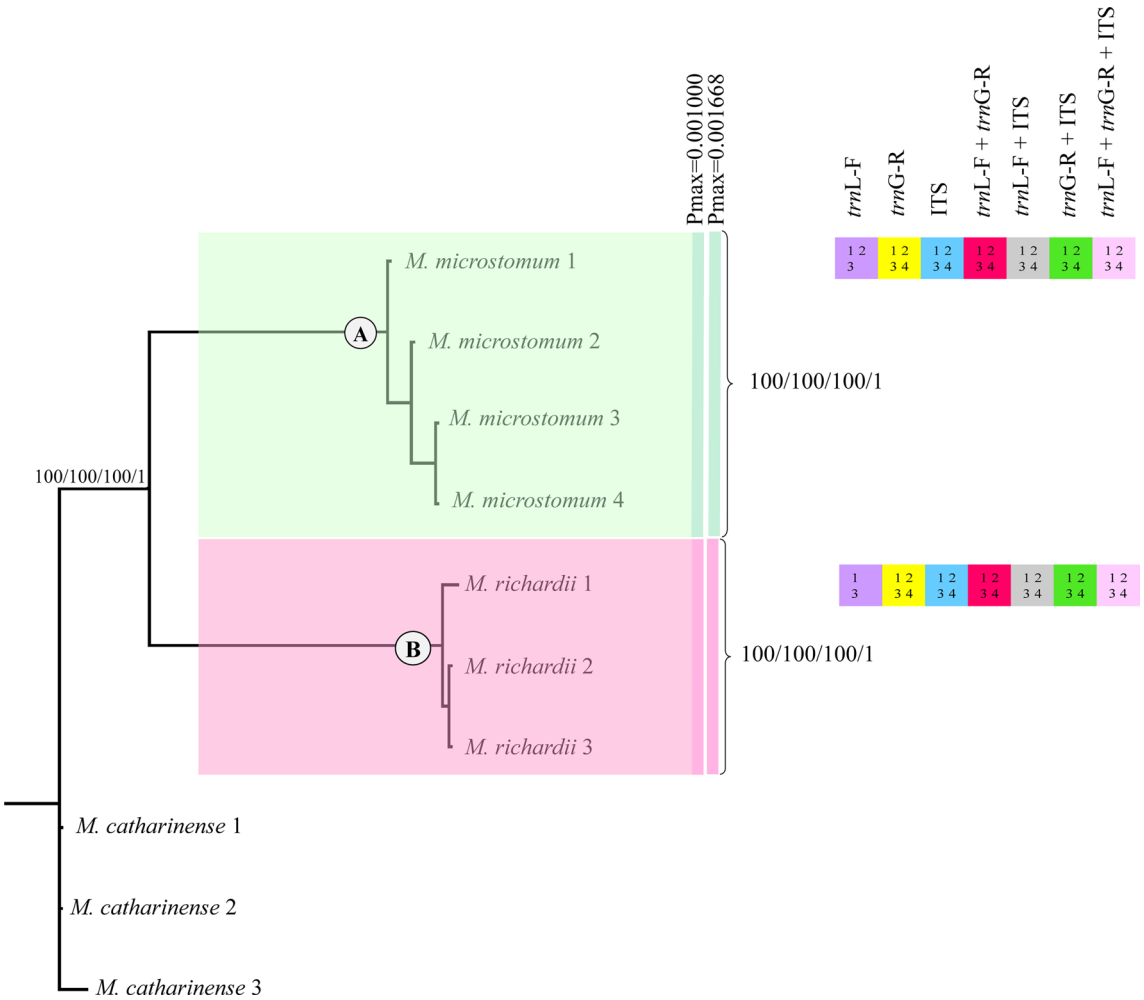

Fig. 3 Phylogram obtained from Bayesian inference (BI) based on combined trnL-F + trnG-R + ITS sequences of 10 specimens of *Macromitrium* (Group 1), including indels coded by simple indel coding. Bootstrap support for Neighbor-joining (NJ), Maximum Parsimony (MP), Maximum Likelihood (ML) and Bayesian posterior probabilities is shown in each clade and node. Colored squares, and numbers inside them represent the clades with bootstrap ≥ 70% for 1—(NJ), 2—(MP) and 3—(ML), and Posterior Probability ≥ 0.95 for 4—(BI). Each colored square represents an analysis of a single marker or combinations of them. The absence of color means no support or clades not resolved for that marker. ABGD species clusters with different Pmax-values are shown next to the species names. Each color represents one species

of species discriminated with high support were 86% (ML), 72% (BI) and 43% (NJ, MP), respectively. For MG1, ML analysis discriminated both species with maximum support, whereas with NJ, MP and BI analysis received lower support or not support.

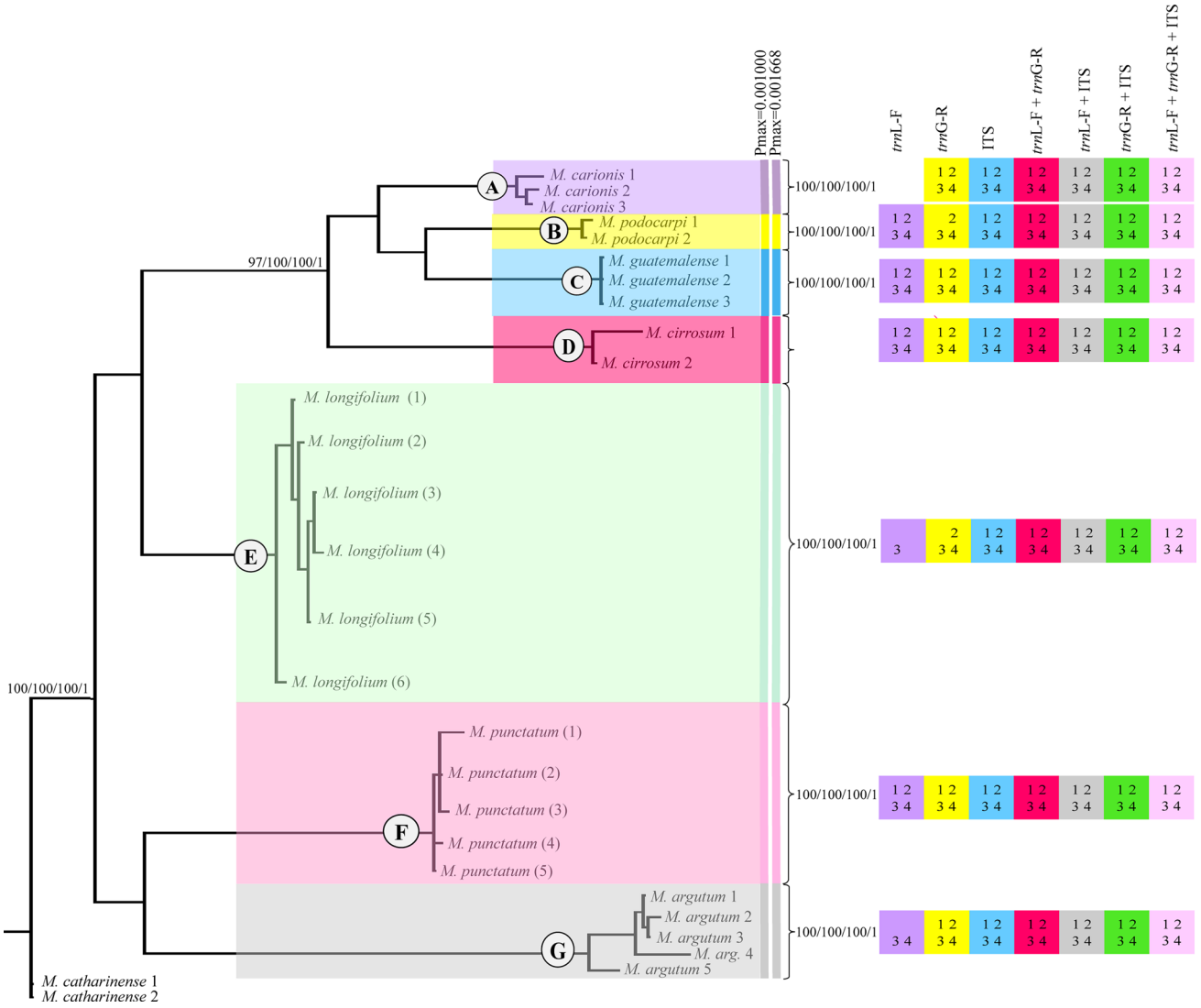

Fig. 4 Phylogram obtained from Bayesian inference (BI) based on combined trnL-F + trnG-R + ITS sequences of 28 specimens *Macromitrium* (Group 2), including indels coded by simple indel coding. Bootstrap support for Neighbor-joining (NJ), Maximum Parsimony (MP), Maximum Likelihood (ML) and Bayesian posterior probabilities are shown in each clade and node. Colored squares, and numbers inside them represent the clades with bootstrap ≥ 70% for 1—(NJ), 2—(MP) and 3—(ML), and Posterior Probability ≥ 0.95 for 4—(BI). Each colored square represents an analysis of a single marker or combinations of them. The absence of color means no support or clades not resolved for that marker. ABGD species clusters with different Pmax-values are shown next to the species names. Each color represents one species

The use of indels significantly increased clade support in MP and BI analyses of *trn*G-R for MG2 (Table 6). Maximum parsimony BS for clades B and E raised from 66 to 90% and from 62 to 94%, respectively. Furthermore, both clades obtained maximum Bayesian support. For MG1 the use of indels resulted in a decrease of BS for the ITS marker and the combinations *trn*L-F + ITS in ML analyses (data not shown).

Ranges of interspecific versus intraspecific pairwise nucleotide distances according to the K2P model are shown in Tables 7. No overlap between the maximum intraspecific and minimum interspecific distance was present in MG1, whereas in MG2 there was small overlap (0.002) between *Macromitrium guatemalense* and *M. podocarpi* in ITS.

The species delimitation method ABGD revealed a clear "barcode gap" in two partitions at Pmax = 0.0010 and Pmax = 0.0016, delimiting seven putative species clusters in MG2 (Fig. 4). For MG1, four partitions with Pmax = 0.0010, 0.0016, 0.0027 and 0.0046, all delimiting two putative species clusters, were found, of which the first and second partitions are shown in Fig. 3.

Table 5 *Macromitrium* (Group 1)

Clade	*trn*L-F				*trn*G				ITS				*trn*L-F + *trn*G			*trn*L-F + ITS			*trn*G + ITS				*trn*L-F + *trn*G + ITS					
	NJ	MP	ML	BI	NJ	MP	ML	BI	NJ	MP	ML	BI	NJ	MP	ML	BI	NJ	MP	ML	BI	NJ	MP	ML	BI	NJ	MP	ML	BI
M. microstomum	73	71	100	–	100	100	100	1	100	100	90	1	100	100	100	1	100	100	92	1	100	100	100	1	100	100	100	1
M. richardii	70	69	100	–	100	100	100	1	100	100	100	1	100	100	100	1	100	100	100	1	100	100	100	1	100	100	100	1

Bootstrap values (%) for analysis of Neighbor joining (NJ) using 2-parameter (K2P) model, Maximum Parsimony (MP), and Maximum Likelihood (ML). For Bayesian Inference (BI) are shown Posterior probability. Every analysis was performed for individual and combined markers. For the combined analysis of all three markers the support is shown in Fig. 3. To NJ, MP and ML were considered bootstrap ≥ 70% and ≥ 0.95 to BI. MP, ML and BI without IndelCoder

Table 6 *Macromitrium* (Group 2)

Clade	*trn*L-F				*trn*G				ITS				*trn*L-F + *trn*G			*trn*L-F + ITS			*trn*G + ITS			*trn*L-F + *trn*G + ITS							
	NJ	MP	ML	BI	NJ	MP	ML	BI	NJ	MP	ML	BI	NJ	MP	ML	BI	NJ	MP	ML	BI	NJ	MP	ML	BI	NJ	MP	ML	BI
M. *argutum*	63	62	100	0.97	100	100	100	1	100	100	100	1	100	100	100	1	100	100	100	1	100	100	100	1	100	100	100	1
M. carionis	–	–	–	–	96	98	99	1	100	100	99	1	96	98	98	1	97	100	100	1	100	100	100	1	100	100	100	1
M. cirrosum	98	97	100	1	100	100	99	1	?	?	?	?	100	100	100	1	?	?	?	?	?	?	?	?	?	?	?	?
M. guatemalense	99	100	100	1	100	100	100	1	100	100	100	1	100	100	100	1	100	100	100	1	100	100	100	1	100	100	100	1
M. *longifolium*	62	62	100	–	63	94	99	1	100	100	95	1	86	98	99	1	100	100	99	1	100	100	100	1	100	100	100	1
M. podocarpi	93	93	100	1	64	90	99	1	100	100	100	1	96	99	100	1	100	100	100	1	100	100	100	1	100	100	100	1
M. *punctatum*	98	99	100	1	100	100	100	1	100	100	100	1	100	100	100	1	100	100	100	1	100	100	100	1	100	100	100	1

Bootstrap values (%) for analysis of Neighbor joining (NJ) using 2-parameter (K2P) model, Maximum Parsimony (MP), and Maximum Likelihood (ML). For Bayesian Inference (BI) are shown Posterior probability. Every analysis was performed for individual and combined markers. For the combined analysis of all three markers the support is shown in Fig. 4. To NJ, MP and ML were considered bootstrap ≥ 70% and ≥ 0.95 to BI. P, ML and BI with IndelCoder

Table 7 Intra- versus interspecific pairwise distances of individual markers (*trn*L-F, *trnG-R* and ITS) and combined markers (*trn*L-F + *trnG-R*, *trn*L-F + ITS, *trnG-R* + ITS and *trn*L-F + *trnG-R* + ITS) in Group 1 and Group 2

		*trn*L-F	*trnG-R*	ITS	*trn*L-F + *trnG-R*	*trn*L-F + ITS	*trnG-R* + ITS	*trn*L-F + *trnG-R* + ITS)
MG1	Intra	0 – 0.003	0 – 0.004	0 – 0.022	0 – 0.004	0 – 0.006	0 – 0.006	0 – 0.005
	Inter	0.008 – 0.010	0.034 – 0.038	0.109 – 0.114	0.025 – 0.028	0.072 – 0.075	0.070 – 0.074	0.056 – 0.060
	Overlap	–	–	–	–	–	–	–
MG2	Intra	0 – 0.003	0 – 0.003	0 – 0.019	0 – 0.002	0 – 0.003	0 – 0.003	0 – 0.002
	Inter	0.005 – 0.029	0.010 – 0.035	0.017 – 0.120	0.011 – 0.031	0.005 – 0.029	0.010 – 0.034	0.011 – 0.031
	Overlap	–	–	0.002	–	–	–	–

4 Discussion

Circumscription of Macromitrium – According to Sharp et al. (1994) the diagnostic morphological characters of *Macromitrium* are: plants light-to-dark green; leaf cells flat or bulging, smooth to papillose-tuberculate below; peristome usually rudimentary, single or, if double, fused to form membranes; calyptra conic, short, with numerous lobes and more or less laciniate, plicate. But there are no characters shared by all *Macromitrium* species. This difficult morphological circumscription may indicate that *Macromitrium* is not monophyletic, which was already suggested by Goffinet et al. (1998) and Frey and Stech (2009). The present phylogenetic data confirm that Brazilian *Macromitrium* species

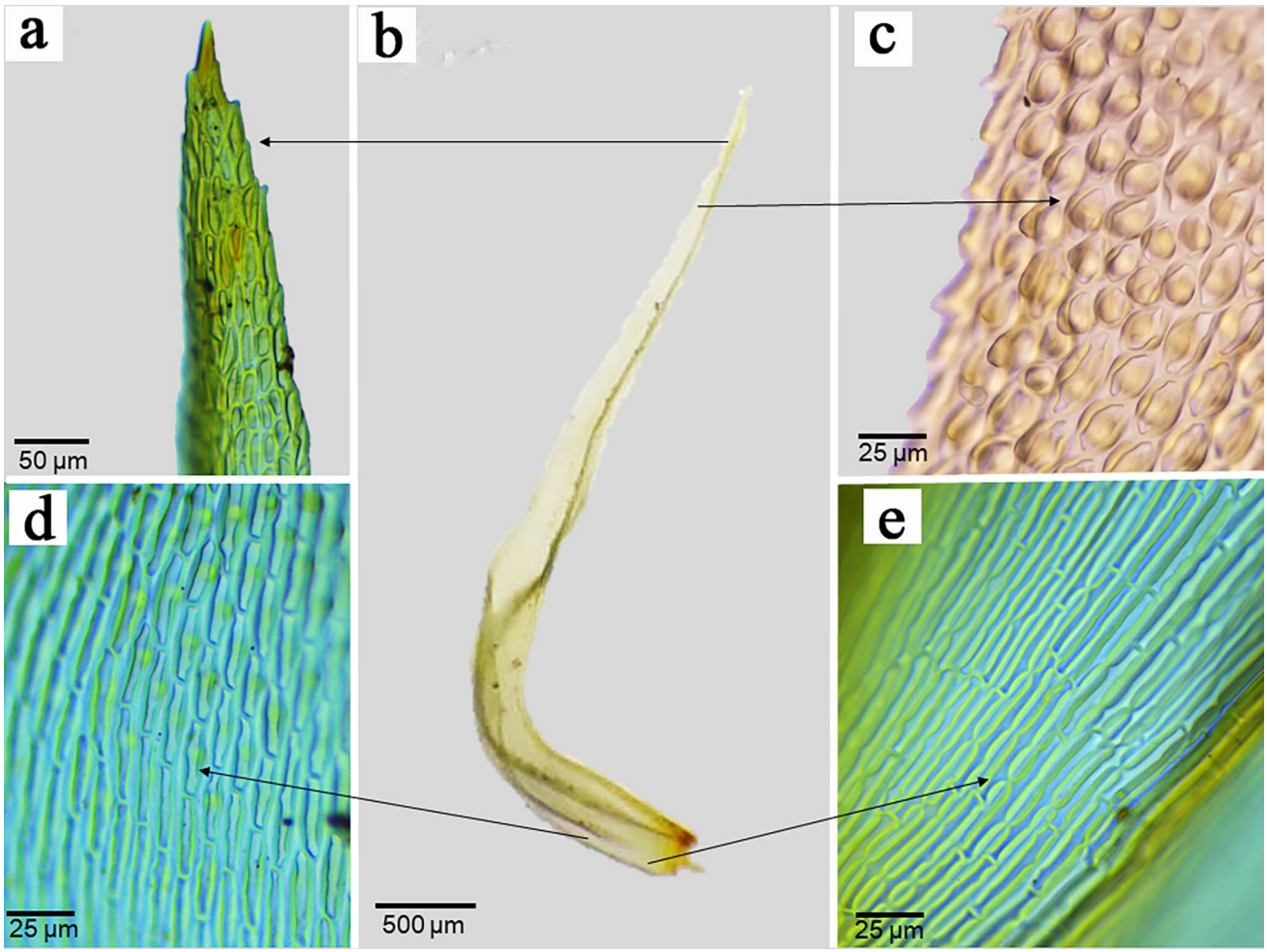

Fig. 5 *Macromitrium catharinense:* (**A**) margin and apex format; (**B**) leave; (**C**) pluripapillose cells; (**D**) pluripapillose base cells; (**E**) base cell

Table 8 Morphological characters used to discriminate between the species of *Macromitrium* and *Pseudomacromitrium*

Caracteres	*Macromitrium*		*Pseudomacromitrium*							*Aureomacromitrium*
	A *M. microstomum*	B *M. richardii*	A *M. carionis*	B *M. podocarpi*	C *M. guatemalense*	D *M. cirrosum*	E *M. longifolium*	F *M. punctatum*	G *M. argutum*	A *M. catharinense*
Leaves format	Lanceolate to ligulate-lanceolate	Lanceolate to ligulate-lanceolate	Lingulate to ovate-lingulate	Lanceolate	Lanceolate to ovate-lanceolate	Linear-lanceolate	Lanceolate	Lanceolate	Lanceolate	Narrow-lanceolate
Apex margin	Entire	Crenulate	Entire	Entire or crenulate	Serrulate	Serrulate to irregularly serrulate above	Entire	Slightly serrulate	Strongly serrulate	Serrulate above
Apex format	Acute or short-acuminate	Acute, obtuse, or obtusely mucronate	Rounded-obtuse, emarginate to mucronate	Acute to obtusely apiculate	Acute or rarely broadly acute	Lanceolate	Acute to acuminate	Acute to acuminate	Acute	Acuminate finished in few elongated cells
Apex cells	Isodiametric smooth	Isodiametric pluripapillose cells (3–4) papillae	Isodiametric bulging	Isodiametric bulging	Isodiametric bulging	Elliptic to rhomboidal	Isodiametric	Isodiametric bulging	Isodiametric	Isodiametric with a big papilla in each cell
Basal cells format	Linear-rectangular not tuberculate	Smooth, rectangular to long-linear, with thick, unevenly thickened walls	Linear, strongly tuberculate	Linear, strongly tuberculate	Linear, strongly tuberculate	Elongate-rectangular, very thick-walled, tuberculate cells	Slightly tuberculated	Slightly tuberculated	Slightly tuberculated	Linear, long-rectangular, incrassate and porose, smooth
Base margin	Inflated long-linear, non-tuberculate	Inflated long-linear, non-tuberculate	Tuberculate projections	Inflated long-linear, non-tuberculate	Cells tuberculate, with up to 20 thin-walled cells at basal margins with ends projecting as blunt teeth	Thin-walled, hyaline, rectangular cells forming an entire basal border	Inflated long-linear, non-tuberculate	Inflated long-linear, non-tuberculate	Inflated long-linear, non-tuberculate	Inflated long-linear, non-tuberculate

are indeed polyphyletic and split into at least three different clades (MG1, MG2 and MG3). Extended studies of further *Macromitrium* species from other geographic areas should reveal whether all species can be assigned to one of these three clades, or whether more separate lineages are to be discovered.

Clade MG1 includes the type species, *M. pallidum* (Fig. 2), and is thus considered *Macromitrium* s.str. This group is sister of *Desmotheca* (Fig. 1), as previously reported by Goffinet et al. (1998) for *M. richardii*. We suggest to maintain both groups as separate genera due to their substantial morphological differences, as *Desmotheca* differs from *Macromitrium* by totally lacking a peristome, very short setae, and enlarged, sheathing, ligulate perichaetial leaves. The oblong, apiculate branch leaves with isodiametric cells are also characteristic of *Desmotheca* (Vitt 1990).

The second clade MG2 is formed by the majority of the species recognized as *Macromitrium* in Brazil. Its sister group relationship with *Groutiella* was already shown by Goffinet et al. (1998) for *M. longifolium* (Hook.) Brid., *Groutiella chimborazensis* (Spruce ex Mitt.) Florsch. and *G. apiculata* (Hook.) H.A. Crum & Steere. Despite their close phylogenetic relationship, *Groutiella* differs from *Macromitrium* by the marginal limbidium of hyaline elongate cells and a short calyptra covering only the upper portion of the urn (Goffinet et al. 1998). In addition, the species belonging to MG2 have tuberculate basal cells, whereas *Groutiella* always has smooth basal cells (Gradstein et al. 2001). Based

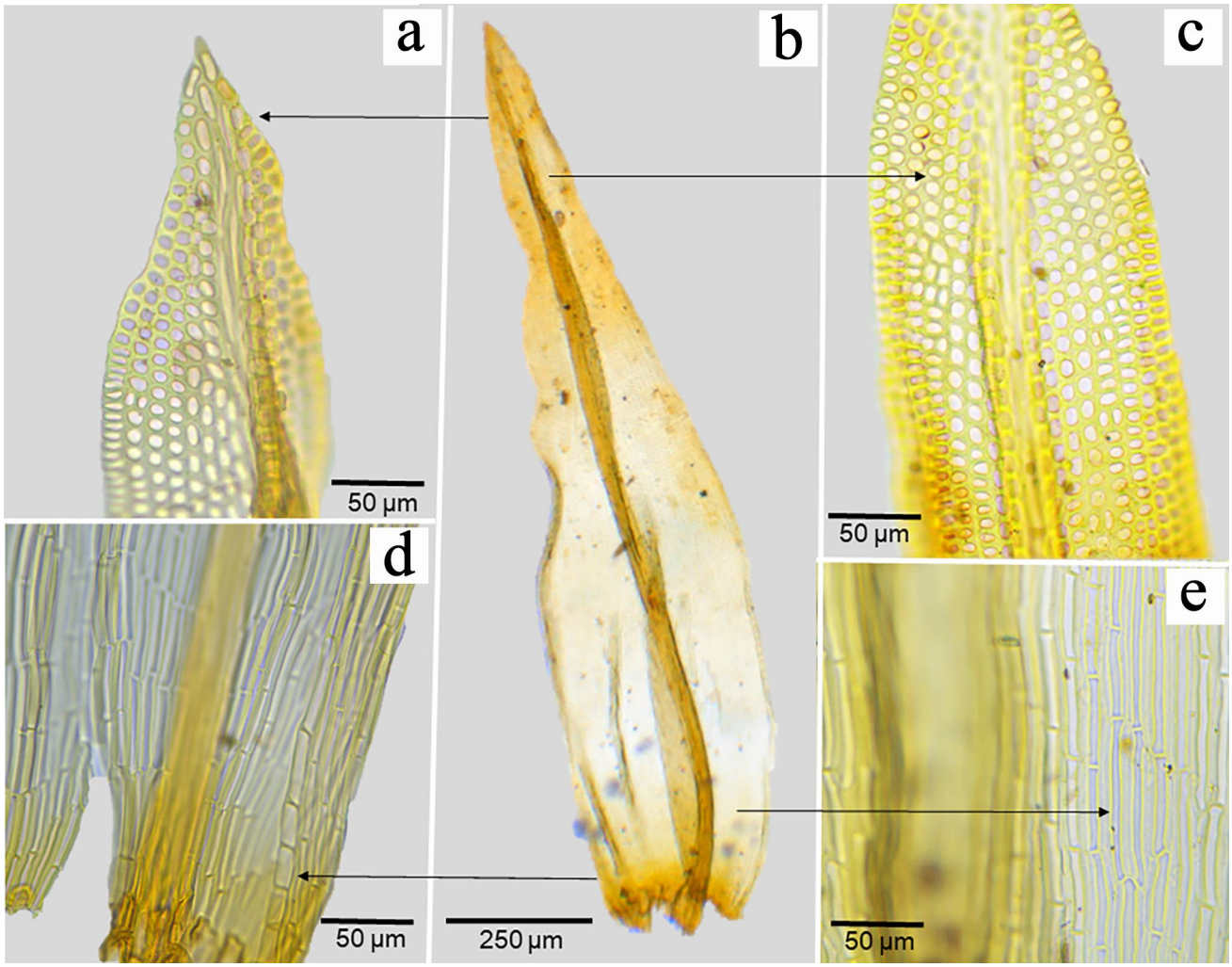

Fig. 6 *Macromitrium microstomum;* (**A**) margin and apex format; (**B**) leave; (**C**) pluripapillose apical cells; (**D**) base margin; (**E**) base cell

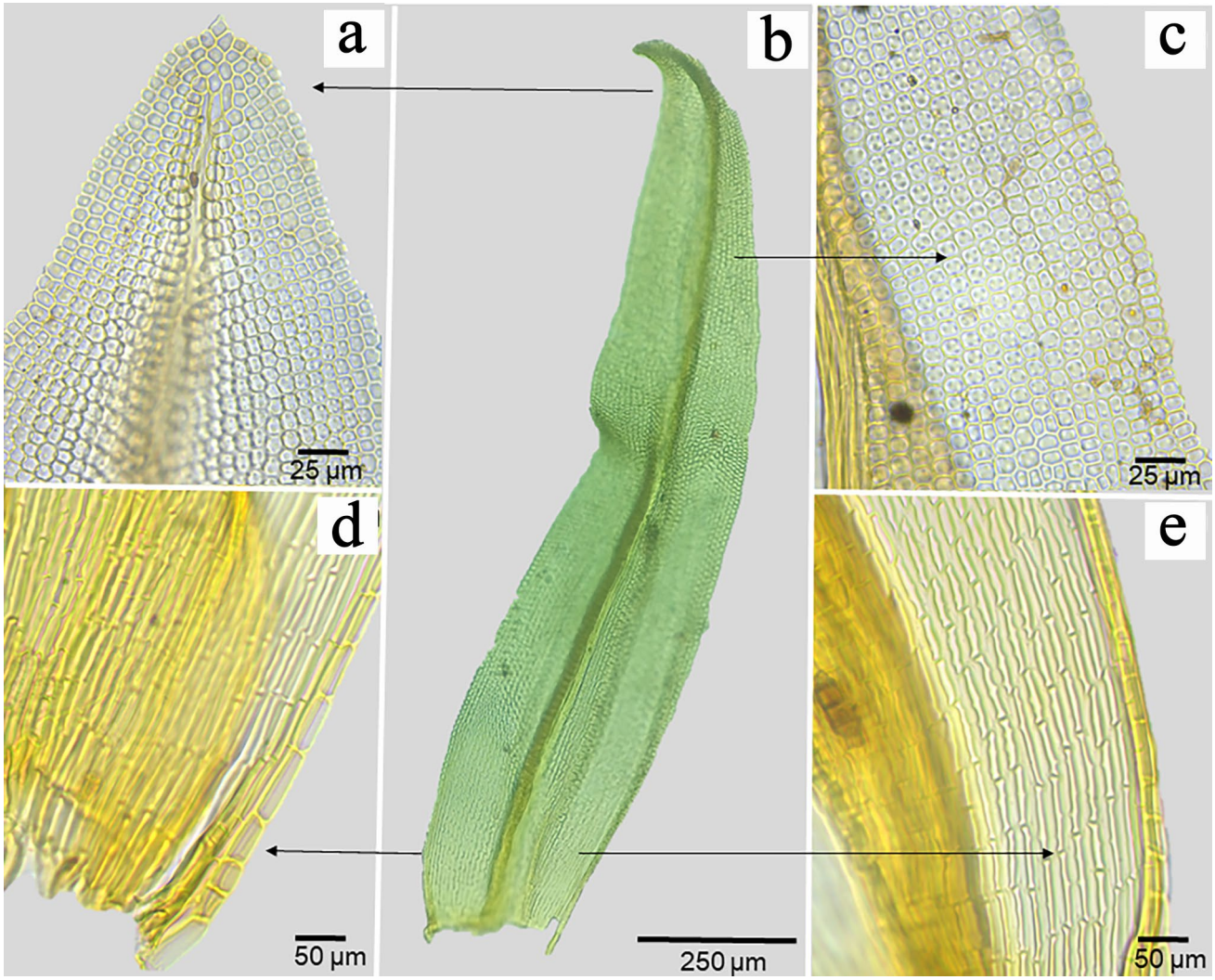

Fig. 7 *Macromitrium richardii;* (**A**) margin and apex format; (**B**) leave; (**C**) apex cells; (**D**) base margin; (**E**) base cell

on the morphological differences between the two groups we suggest to keep them as separate genera, and to describe the new genus *Pseudomacromitrium* for the MG2 clade.

The MG3 clade, formed only by *M. catharinense*, had maximum support in all analyses. It appeared sister to the *Groutiella—Pseudomacromitrium* (MG2) clade, albeit with high support only under Bayesian inference. *Macromitrium catharinense* (Fig. 5; Table 8) has a very different morphology: leaves larger (up to 4 mm) than the species of *Macromitrium, Groutiella* and *Pseudomacromitrium* (up to 2 mm), papillose upper leaf cells and smooth basal cells. Due to the morphological characteristics and molecular results, we describe a new genus *Aureomacromitrium* for *M. catharinense*.

Molecular species discrimination (DNA barcoding) – For Brazilian *Macromitrium* (MG1) and *Pseudomacromitrium* (MG2) the *trn*G-R region presented the best results. The *trn*G-R region is easy to amplify, with amplicons ranging from 734 to 744 base pairs in the sequenced specimens, excellent sequence quality, easy to align and with sufficient variability to identify 100% of the species of MG1

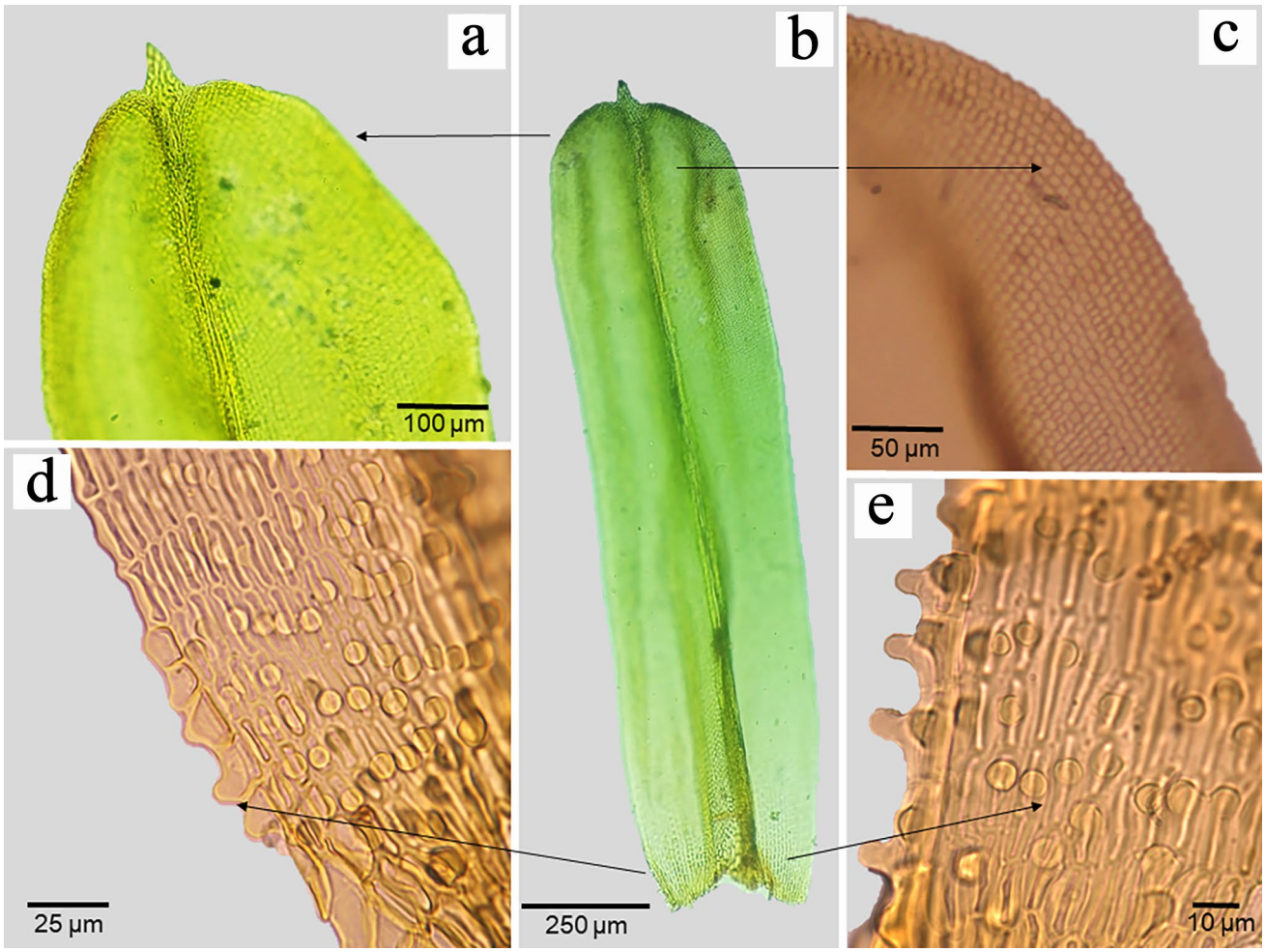

Fig. 8 *Macromitrium carionis;* (**A**) margin and apex format; (**B**) leave; (**C**) apex cells; (**D**) base margin; (**E**) base cells

and MG2. Usually for bryophytes only the *trn*G intron has been used (e.g., Câmara and Shaw 2013; Carter 2010, 2012; Hedenäs 2009; Medina et al. 2013). Li et al. (2013) tested the *trn*G intron for the identification of Chinese *Macromitrium* species, presenting discrimination potential for 86% of the species, 14% less variation compared to the intergenic *trn*G-*trn*R spacer used in this study. For the genus *Schlotheimia*, the *trn*G-R region discriminated 100% of the species, demonstrating that the addition of the *trn*G-*trn*R intergenic spacer significantly increases the discrimination potential (Valente et al. 2019). The *trn*G-R region has also been used successfully for phylogenetic inference (Nagalingum et al. 2007; León et al. 2013) and DNA barcoding of ferns (Pryer et al. 2010), and we suggest to employ the same region in future studies of bryophytes as well, instead of only the *trn*G intron.

The ITS marker was easy to amplify and highly variable, allowing for 100% discrimination of the MG1 and MG2 species. However, due to the large interspecific variation, it was very difficult to perform the sequence alignment for both groups together. Compared to *Schlotheimia* (Valente et al. 2019), the ITS sequences of MG1 and MG2 were more conserved, presenting 5.7 and 2.4% less informative sites, respectively. However, the sequences of MG1 and MG2 presented higher quality in relation to the genus *Schlotheimia* due to the lack of poly-C, -T and -A nucleotide stretches in ITS1, which were prominent in the latter genus (Valente et al. 2019). In addition, ITS sequencing is prone to fungal contamination (e.g., Hollingsworth et al. 2011; Valente et al. 2019).

The *trn*L-F region was also easy to amplify and sequence quality was high, as in earlier DNA barcoding studies of bryophytes (e.g., Liu et al. 2010; Valente et al. 2019). The species discrimination capacity of *trn*L-F, however, varied considerably in different bryophyte genera, from 53% in *Dicranum* Hedw. (Lang et al. 2014) to 89% in 49 species

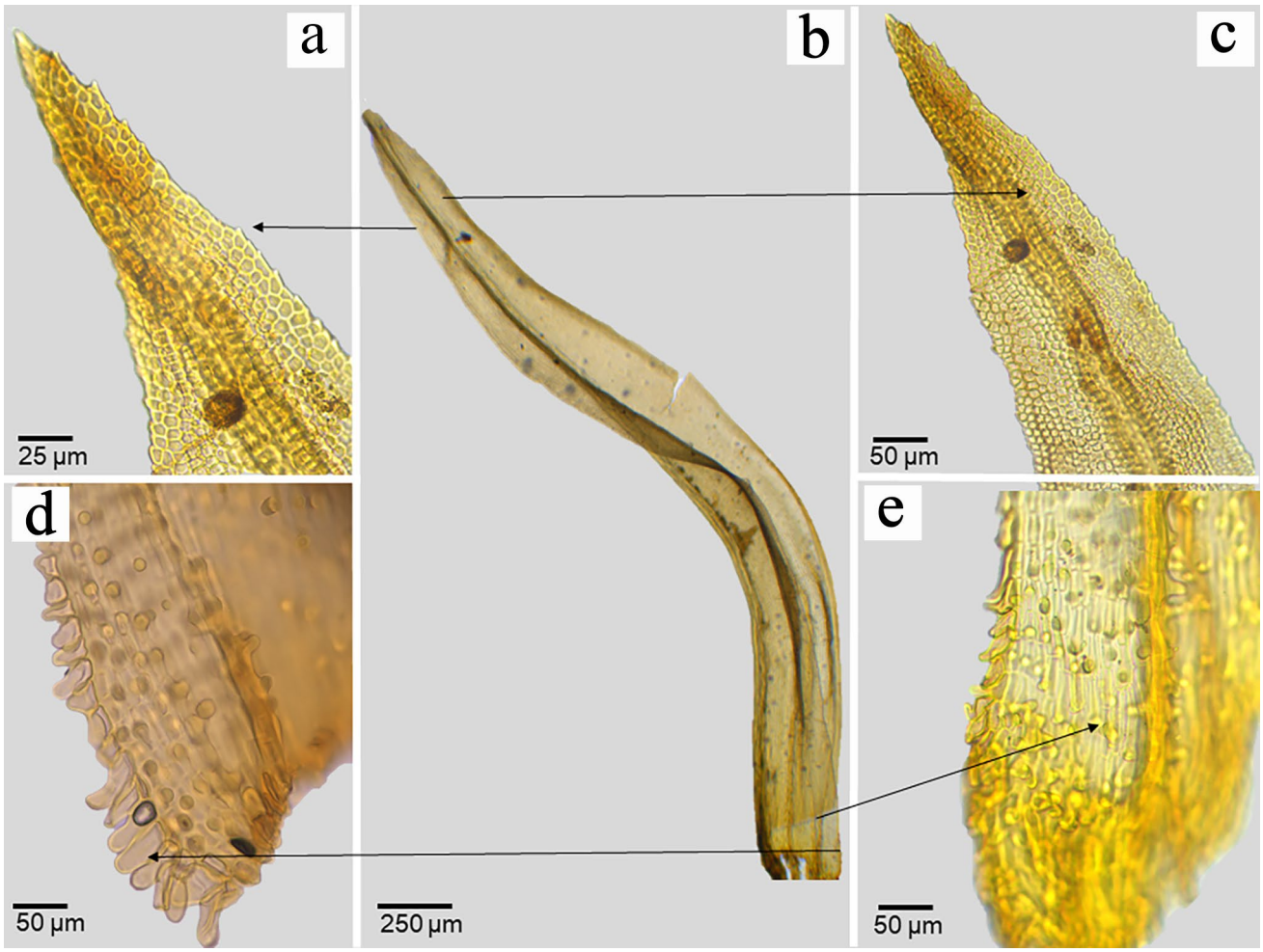

Fig. 9 *Macromitrium guatemalense;* (**A**) margin and apex format; (**B**) leave; (**C**) apex cells; (**D**) base margin; (**E**) base cells

of mosses (Liu et al. 2010). In Orthotrichaceae, this marker alone was able to discriminate only 57% of the Chinese species of *Macromitrium* (Li et al. 2013), and in Brazilian *Schlotheimia* the discrimination potential was even lower, 45% (Valente et al. 2019). For the Brazilian *Macromitrium* s.l. species, the discrimination capacity was 43%.

With the exception of *trn*L-F, all other markers and combinations were efficient to be used as barcoding markers for the identification of Brazilian *Macromitrium* s.l. species. However, by comparing the characteristics of each marker (amplification rate, variability, sequence quality) costs and laboratory time, we suggest *trn*G-R as core barcoding marker for routine identification of all Brazilian species.

The intraspecific variation of *M. argutum* is greater than the interspecific variation between *M. podocarpi* and *M. guatemalense,* which leads to overlap of intra- and interspecific distances in ITS (Group 1 in Table 7). However, the clades of all species are well supported and the recognition of *M. argutum* is supported by ABGD, indicating that an overall comparison of pairwise distances is less meaningful than the phylogenetic and species delimitation methods. Our ABGD results, suggesting the delimitation of two species in MG1 and seven species in MG2, corroborate the results of tree-based analyses. The ABGD method presented congruent results with other discrimination methods for the delimitation of *Macromitrium* species and for other groups of bryophytes, like *Aneura* Dumort. (Metzgeriales) (Bączkiewicz et al. 2017), *Schistidium* Bruch & Schimp. (Grimmiaceae) (Biersma et al. 2018) and *Bartramia* Hedw. (Bryophyta) in Antarctica (Câmara et al. 2019).

Diagnostic morphological characters – To corroborate the molecular data, we present a set of morphological characters (Table 8) and illustrative figures to aid in the morphological identification of the Brazilian species of *Aureomacromitrium*

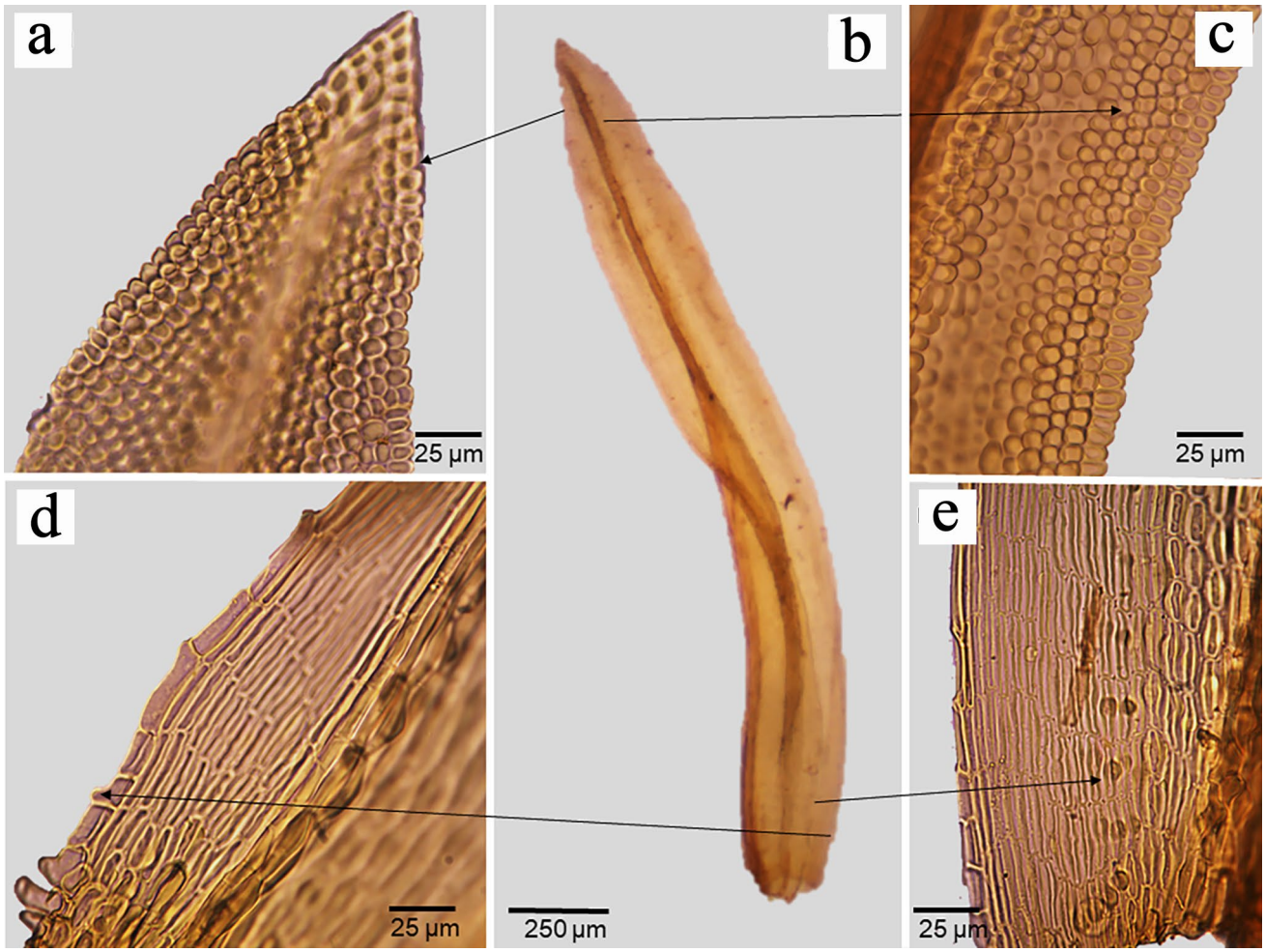

Fig. 10 *Macromitrium podocarpi;* (**A**) margin and apex format; (**B**) leave; (**C**) apex cells; (**D**) base margin; (**E**) base cells

(Fig. 5, see discussion above), *Macromitrium* (Figs. 6, 7) and *Pseudomacromitrium* (Figs. 8, 9, 10, 11, 12, 13 and 14).

Brazilian *Macromitrium* species differ from *Pseudoacromitrium* mainly in that they do not have tuberculate cells at the base of the leaves. Both species of *Macromitrium* differ from each other by unipapillose upper lamina cells in *M. microstomum* (Fig. 6) versus pluripapillose cells with 3–4 papillae on each cell in *M. richardii* (Fig. 7; Allen 2002).

The Brazilian species of *Pseudomacromitrium* can be distinguished from each other by combinations of four morphological characters of the leaf, namely (1) leaf base margins, (2) basal lamina cells, (3) apex shape and (4) apex margins (Table 8).

Pseudomacromitrium carionis (Fig. 8) and *P. guatemalense* (Fig. 9) both have swollen teeth on the basal leaf margins and strongly tuberculate cells; however, the specimens of *P. carionis* have a rounded-obtuse, emarginate to mucronate apex and entire margin, while *P. guatemalense* has an acute or rarely broadly acute apex and serrulate margins.

The other *Pseudomacromitrium* species do not have teeth at the basal margin but present well inflated rectangular and/or quadratic cells, two or three times wider than the inner basal lamina cells. *Pseudomacromitrium podocarpi* (Fig. 10) and *P. cirrosum* (Fig. 11) have evident tubercles on the basal lamina. *Pseudomacromitrium podocarpi* is the smallest plant (leaves 1.5–2.2 mm) with acute to obtuse-apiculate apex and entire or crenulate margins, while *P. cirrosum* is larger (leaves up to 3–5 mm) with lanceolate apex and serrulate to irregular serrulate distal margins.

The species *P. longifolium*, *P. punctatum* and *P. argutum* have few tubercles, which are often difficult to detect. The specimens of *P. argutum* (Fig. 12) show acute or lanceolate apex and strongly serrulate margins. The other two species present an acute to acuminate apex and can be distinguished from each other by entire margins at the leaf apex and upper lamina cells of each leaf not bulging (*P. punctatum*, Fig. 13). The clade F (Fig. 14) presents a slightly serrulate margin apex and cells bulging upper leaves (*P. argutum*).

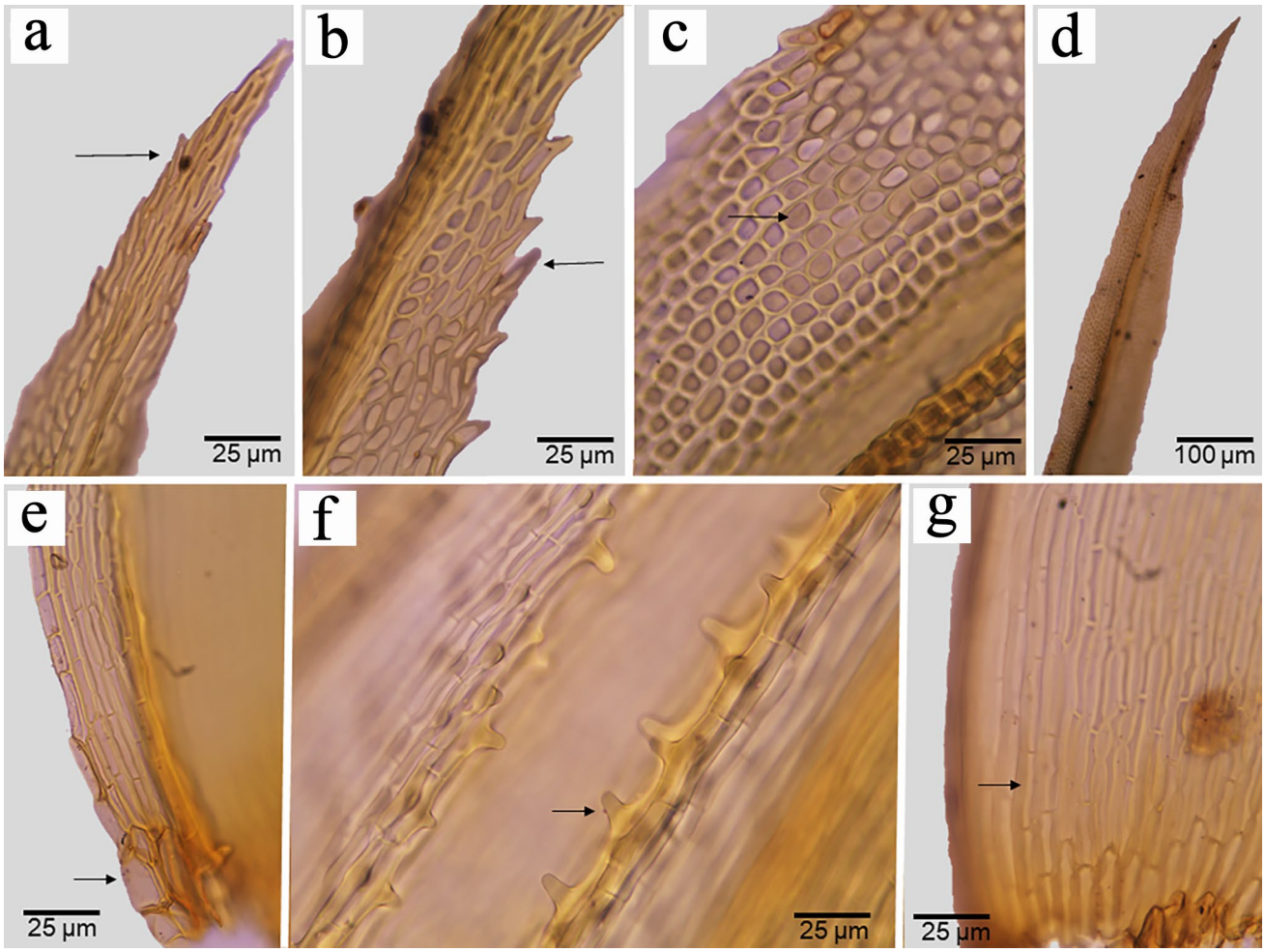

Fig. 11 *Macromitrium cirrosum;* (**A**) apex format; (**B**) apex margin; (**C**) apex cells; (**D**) upper leave; (**E**) base margin; (**F**) tubercles; (**G**) base cells

5 Taxonomic treatment

Aureomacromitrium **D.V. Valente, P.E.A.S. Câmara & D.F. Peralta gen. nov.** – Type: *Aureomacromitrium catharinense* (Paris) D.V. Valente, P.E.A.S. Câmara & D.F. Peralta.

Plants robust, yellow-green, yellow, yellowish brown in old stems. Prostrate stems with ascending branches. Narrow-lanceolate leaves, contorted or crisped when dry, and erect to undulate when wet; apex acuminate finished in few elongated cells; costae single, percurrent, or excurrent; margins serrate to serrulate above, entire below; upper cells isodiametric to gradually rectangular at median lamina, with a big tuberculate papilla on each cell. Basal cells are linear, long-rectangular, incrassate and porose, smooth. Cladocarpous. Capsules oblong, exserted; peristome double, exostome rudimentary, with truncated teeth, endostome of 16 teeth deeply divided, with fused segments. Spores globular. Calyptra cucullate, with many hairs.

Etymology The name is linked with the fact that the type species presents a golden coloration in nature.

Distribution Occurs in Brazil, Colombia and Ecuador.

Aureomacromitrium catharinense **(Paris) D.V. Valente, P.E.A.S. Câmara & D.F. Peralta comb. nov. ≡** ***Macromitrium catharinense*** **Paris, Index Bryologicus Supplementum Primum 237. 1900,** ***nom. nov.*** **for** ***M. prolongatum*** **Müll.Hal., Bull. Herb. Boissier 6: 99 (1898), hom. illeg.** – TYPE: Brasilia, Serra Itatiaia 2000 m. alt., Martio 1894, sterile, [E. Ule] N° 1835 (Lectotype H designated by Li et al. (2019) [hb.Brotherus]—barcode H2649005; isolectotypes FI, GOET barcode GOET012311, JE barcodes JE04006251, JE04006252, PC barcodes PC0137901, PC0137902, PC0137903, PC0137904, MICH barcode MICH525906, NY barcode NY01202245, L!); [Brazil] Sa. Catharina, Serra Geral, in ramis arborum, Januario 1890, cum fructibus junioribus, [E. Ule] N° 847 (Syntype FI); [Brazil] ad ramos arborum

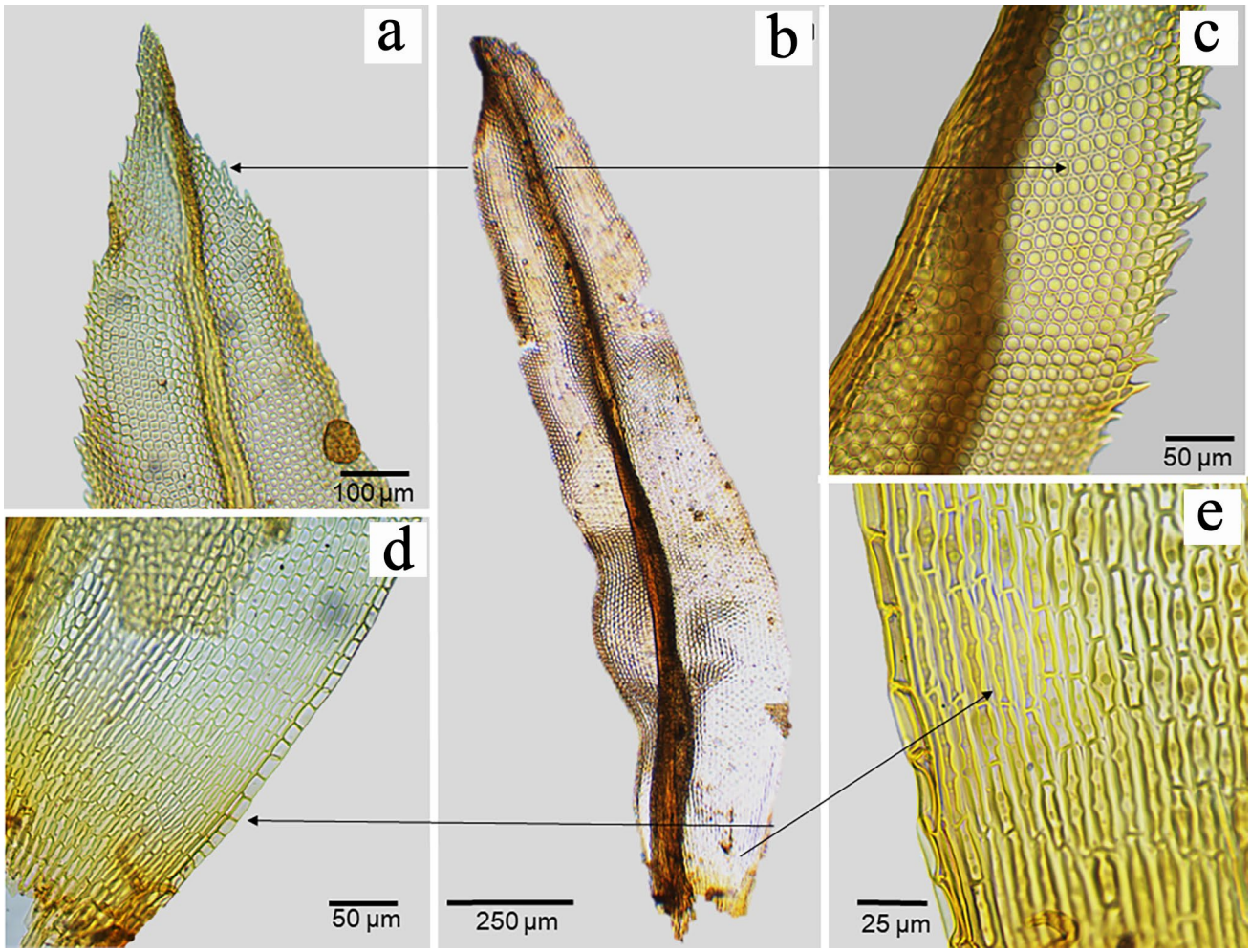

Fig. 12 *Macromitrium argutum;* (**A**) margin and apex format; (**B**) leave; (**C**) apex cells; (**D**) base margin; (**E**) base cells

marginis Serae ejusdem, Aprili 1891 cum fructu vetusta et ramis aureis, [E. Ule] N° 1017 (?). (Fig. 5: A-E).

Pseudomacromitrium **D.V. Valente, P.E.A.S. Câmara & D.F. Peralta gen. nov.** – Type: *Pseudomacromitrium podocarpi* (Müll.Hal.) D.V. Valente, P.E.A.S. Câmara & D.F. Peralta.

Plants small, medium-sized to robust, mats or cushions on trees or rocks. Primary stems creeping, secondary stems erect-ascending, tomentose. Leaves plicate, erect-appressed, keeled, erect below, spirally twisted or crisped when dry, erect to flexuose-spreading when wet, 1.5–5 mm long, lingulate, oblong-lanceolate or lanceolate; apices rounded, obtuse emarginate or short-mucronate, acuminate, acute to obtuse-apiculate; costae strong, subpercurrent, percurrent, or excurrent; margins entire, crenulated, serrate to serrulate, undulate, erect to plane above, recurved or plane below, enlarged basal teeth at leaf insertion present or absent; upper cells 5–15 µm, rounded-quadrate, rhombic, rounded-hexagonal, smooth, bulging to mamillose, upper marginal cells not differentiated, basal cells linear, long-rectangular 16–60 µm, incrassate and porose, weakly or strongly tuberculate. Autoicous, dioicous or pseudautoicous. Setae 3–15 mm long, smooth or papillose. Capsules 1–2.5 mm long, ovoid, oblong, cylindrical, plicate or furrowed. operculum conic-rostrate to rostrate, 1–1.5 mm long; annulus non-revoluble, with fragments adhering to capsule mouth; exostome teeth truncate or lanceolate 160–312 µm high, papillose or papillose-striate, not fused or united and forming an erect membrane; endostome hyaline, papillose to weakly papillose, basal membrane 50–280 µm high, segments rudimentary, present or absent; anisosporous, ornamentation smooth or papillose. Calyptra mitrate, laciniate, naked, with a few hairs or densely hairy, 2.5–4 mm long.

Comments The Brazilian species of *Pseudomacromitrium* differ from *Macromitrium* by having tuberculate cells at the base of the leaves.

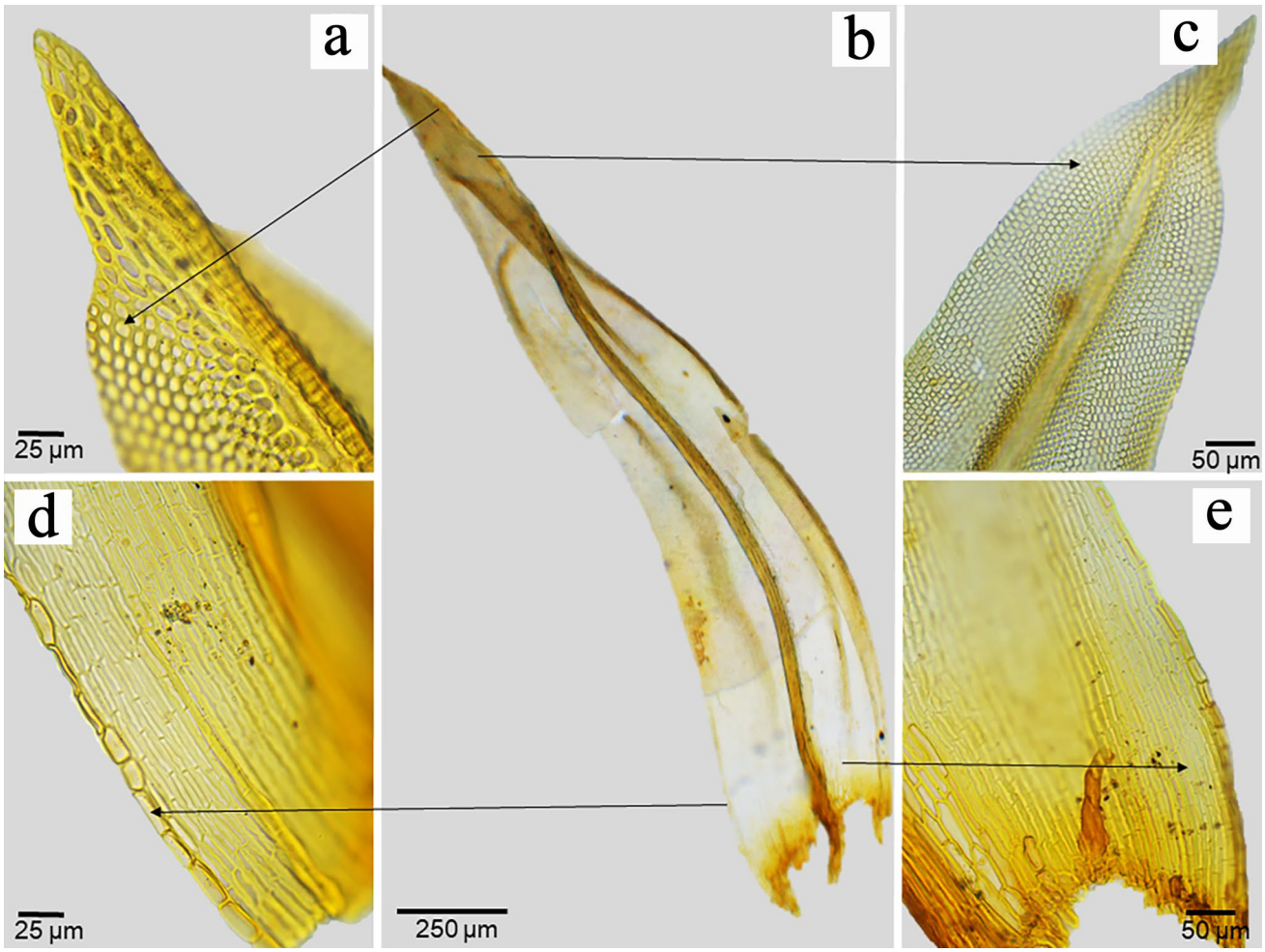

Fig. 13 *Macromitrium longifolium;* (**A**) margin and apex format; (**B**) leave; (**C**) apex cells; (**D**) base margin; (**E**) base cells

Etymology The name is linked with the fact that the species of the genus were so far believed to be part of *Macromitrium*.

Distribution Occurs in Mexico, Central America, Caribbean, Western and Northern South America, Brazil.

***Pseudomacromitrium argutum* (Hampe) D.V. Valente, P.E.A.S. Câmara & D.F. Peralta comb. nov.** ≡ ***Macromitrium argutum* Hampe, Linnaea 22: 581. 1849** – TYPE: [Brazil], Rio de Janeiro, *Glaziou 9241* (lectotype BM designated by Costa et al. (2016) barcode BM000879980!; isolectotypes: BM barcodes BM000879983, BM000879979!).

***Pseudomacromitrium carionis* (Müll.Hal.) D.V. Valente, P.E.A.S. Câmara & D.F. Peralta comb. nov.** ≡ ***Macromitrium carionis* Müll.Hal., Bulletin de l'Herbier Boissier 5: 199. 1897** – TYPE: [Guatemala] Caesta de Lovio, *Bernoulli et Cario 48* (lectotype GOET designated here, barcode GOET011888!; isolectotypes: GOET barcodes GOET012471, GOET012472, GOET011887!, PC barcode PC0137621!) (Fig. 8A–E).

Pseudomacromitrium cirrosum (Hedw.) D.V. Valente, P.E.A.S. Câmara & D.F. Peralta comb. nov. ≡ *Anictangium cirrosum* Hedw., Species Muscorum Frondosorum 42. 5 f. 1–3. 1801.≡ *Hedwigia cirrosa* (Hedw.) Brid., Journal für die Botanik 1800(1):272. 1801. ≡ *Neckera cirrosa* (Hedw.) F.Weber & D.Mohr, Index Musei Plantarum Cryptogmarum 3:1803. ≡ *Anoectangium cirrosum* (Hedw.) Schwägr., Species Muscorum Frondosorum supplementum primum 1:38. 1811.≡ *Schlotheimia cirrosa* (Hedw.) Brid., Muscologia Recentiorum Supplementum 2:19. 1812. ≡ *Orthotrichum cirrosum* (Hedw.) Hook. & Grev., Edinburgh Journal of Science 1:130. 6. 1824. ≡ *Ulota cirrosa* (Hedw.) Hook & Grev., Edinburgh Journal of Science 1:130. 1824. invalid name ≡ *Macromitrium cirrosum* (Hedw.) Brid., Bryologia Universa 1:316. 1826.—TYPE: Jamaica, Montserrat, *sine legit* (holotype: G; isotypes: BM barcode BM000873245; E barcode E00002459). (Fig. 11A–E).

Pseudomacromitrium guatemalense* (Müll.Hal.) D.V. Valente, P.E.A.S. Câmara & D.F. Peralta comb. nov.** ≡ ***Macromitrium

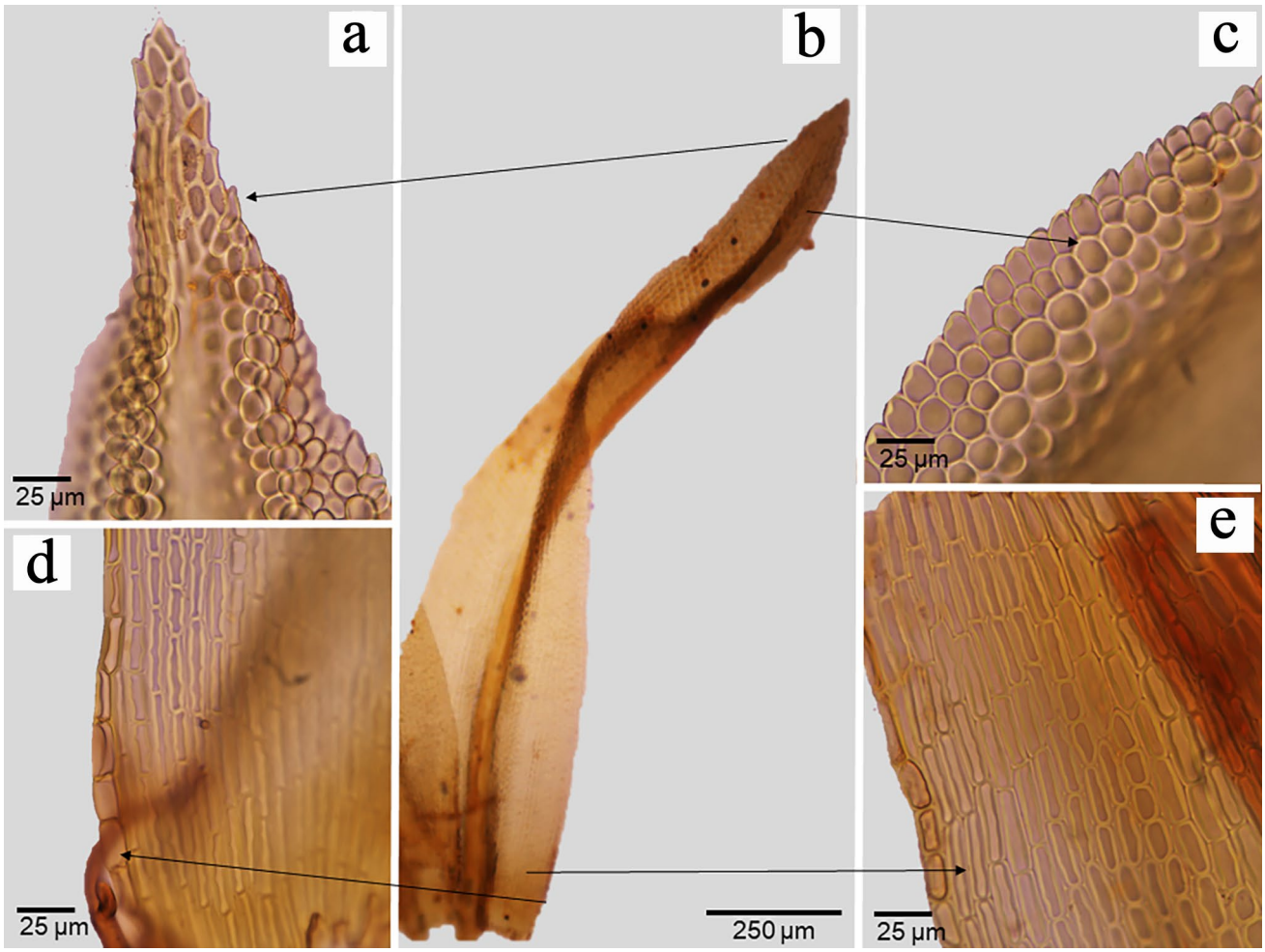

Fig. 14 *Macromitrium punctatum;* (**A**) margin and apex format; (**B**) leave; (**C**) apex cells; (**D**) base margin; (**E**) base cells

***guatemalense* Müll.Hal., Synopsis Muscorum Frondosorum omnium hucusque Cognitorum 2: 644. 1851** – TYPE: Guatemala, Friedrichstal, *Kegel s.n.* (lectotype BM designated here, BM000873191!; isolectotypes: G barcode G00284083!; BM barcode BM000873192!, L barcode L0060440!) (Fig. 9A–E).

Pseudomacromitrium longifolium (Hook.) D.V. Valente, P.E.A.S. Câmara & D.F. Peralta comb. nov. ≡ *Orthotrichum longifolium* Hook., Musci Exotici 1: 44. 1818 ≡ *Macromitrium longifolium* (Hook.) Brid., Bryologia Universa 1: 309, 738. 1826 ≡ *Schlotheimia longifolia* (Hook.) Schwägr., Species muscorum Frondosorum, supplementum secundum 2(2): 147. 1827.—TYPE: [Venezuela] Caracas, *Humboldt et Bonpland s.n.* (lectotype designated by Goffinet (1993) BM barcode BM000873190; isolectotypes: BM barcodes BM000720648, BM000720656!, PC barcodes PC0137790!, PC0137789!, JE barcode JE04008699, E barcode E00289633). (Fig. 13A–E).

***Pseudomacromitrium podocarpi* (Müll.Hal.) D.V. Valente, P.E.A.S. Câmara & D.F. Peralta comb. nov. ≡ *Macromitrium podocarpi* Müll.Hal., Bulletin de l'Herbier Boissier 6: 96. 1898** – TYPE: Brasilia, Minas Gerais, Serra Itabira do Campo, *E. Ule 1066* (lectotype designated here, GOET barcode GOET012309!; isolectotypes: NY barcodes NY01086626!, NY01086627!, G barcodes G00265988!, G00265989!; BM barcode BM000873094!; PC barcode PC0137891!) (Fig. 10A–E).

Pseudomacromitrium punctatum (Hook. & Grev.) D.V. Valente, P.E.A.S. Câmara & D.F. Peralta comb. nov. ≡ *Orthotrichum punctatum* Hook. & Grev., Edinburgh Journal of Science 1: 119. 5. 1824. ≡ *Macromitrium punctatum* (Hook. & Grev.) Brid. Bryologia Universa 1: 739. 1826.—TYPE: Brazil, Raddi *s.n.* (isotypes: E barcodes E00011666!, E00011667!). (Fig. 14A–E).

Obs. We do not choose a lectotype because the original collection of Raddi is in PI.

Supplementary Information The online version contains supplementary material available at https://doi.org/10.1007/s40415-023-00935-3.

Acknowledgements This project was funded by CNPq (Conselho Nacional de Pesquisa—Brasil) Edital 71/2013 (MEC/MCTI/CAPES/CNPq/FAPs), CAPES. We thank the graduate program in Botany at the University of Brasília and Naturalis Biodiversity Center, Leiden, the Netherlands, for hosting the first author as part of her sandwich PhD grant. We thank Elisabeth M. Biersma for helping with the ABGD analyses. We thank Silvia Pressel and Joanna Wilbraham of Natural History Museum, London, United Kingdom, for the *M. pallidum* sequences.

References

Allen BH (2002) Moss flora of Central America. Part 2. Encalyptaceae – Orthotrichaceae. Monogr Syst Bot Missouri Bot Gard 90:viii + 699 pp

Bączkiewicz A, Szczecińska M, Sawicki J, Stebel A, Buczkowska K (2017) DNA barcoding, ecology and geography of the cryptic species of *Aneura pinguis* and their relationships with *Aneura maxima* and *Aneura mirabilis* (*Metzgeriales*, Marchantiophyta). PLoS ONE 12:e0188837. https://doi.org/10.1371/journal.pone.01888

Biersma EM, Jackson JA, Stech M, Griffiths H, Linse K, Convey P (2018) Molecular data suggest long-term in situ Antarctic persistence within Antarctica's most speciose plant genus, Schistidium. Front Ecol Evol 6:77. https://doi.org/10.3389/fevo.2018.00077

Biomatters (2010) Geneious v5.3.6. Available from http://www.geneious.com

Câmara PEAS (2010) Métodos de extração de DNA de Briófitas para estudos filogenéticos. Heringeriana 3:11–17

Câmara PEAS, Shaw AJ (2013) A molecular phylogeny of the moss genus *Taxithelium* (Pylaisidelphaceae) based on plastid, mitochondrial and nuclear markers. Syst Bot 38:861–868. https://doi.org/10.1600/036364413X674832

Câmara PEAS, Soares AER, Henriques DK, Peralta DF, Bordin J, Carvalho-Silva M, Stech M (2019) New insights into the species diversity of *Bartramia* Hedw. (Bryophyta) in Antarctica. Antarct Sci 31:208–215. https://doi.org/10.1017/s0954102019000257

Carter B (2010) The taxonomic status of the Tasmanian endemic moss *Scleropodium australe* (Brachytheciaceae). The Bryol 113:775–780. https://doi.org/10.1639/0007-2745-113.4.775

Carter BE (2012) Species delimitation and cryptic diversity in the moss genus *Scleropodium* (Brachytheciaceae). Mol Phylogenet Evol 63:891–903. https://doi.org/10.1016/j.ympev.2012.03.002

Costa DP, Pôrto KC, Luizi-Ponzo AP, Ilkiu-Borges AL, Bastos CJP, Câmara PEAS, Peralta DF, Bôas-Bastos SBV, Imbassahy CAA, Henriques DK, Gomes HCS, Rocha LM, Santos ND, Siviero TS, Vaz-Imbassahy TF, Churchill SP (2011) Synopsis of the Brazilian moss flora: checklist, distribution and conservation. Nova Hedwigia 93:277–334. https://doi.org/10.1127/0029-5035/2011/0093-0277

Costa DP, Peralta DF, Carvalho-Silva M, Câmara PEAS (2016) Types of the moss names based on Glaziou's collections from Brazil. Taxon 65:839–861. https://doi.org/10.12705/654.10

Cox CJ, Goffinet B, Wickett NJ, Bolesi SB, Shaw AJ (2010) Moss diversity: a molecular phylogenetic analysis of genera. Phytotaxa 9:175–195. https://doi.org/10.11646/phytotaxa.9.1.10

Crosby MR, Magill RE et al (1999) A Checklist of the Mosses. St. Louis, Missouri Botanical Garden

Doyle JJ, Doyle JL (1987) A rapid isolation procedure for small quantities of fresh leaf tissue. Phytochem Bull 19:11–15

Felsenstein J (1985) Confidence limits on phylogenies: an approach using the bootstrap. Evolution 39:779–783. https://doi.org/10.1111/j.1558-5646.1985.tb00420.x

Frey W, Stech M (2009) Marchantiophyta, Bryophyta, Anthocerotophyta. In: Frey W (ed): Syllabus of Plant Families. A. Engler´s Syllabus der Pflanzenfamilien, 13th ed., Part 3 Bryophytes and seedless Vascular Plants. Gebr. Borntraeger, Stuttgart

Goffinet B (1993) Taxonomic and floristic notes on neotropical Macromitrioideae (Orthotrichaceae). Trop Bryol 7:149–154. https://doi.org/10.11646/bde.7.1.11

Goffinet B, Bayer RJ, Vitt DH (1998) Circumscription and phylogeny of the Orthotrichales (Bryopsida) inferred from rbcl sequence analyses. Am J Bot 85:1324–1337. https://doi.org/10.2307/2446642

Goffinet B, Buck WR (2004) Systematics of the Bryophyta (Mosses): from molecules to a new classification. Monogr Syst Bot Missouri Bot Gard 98:205–239

Goffinet B, Vitt DH (1998) Revised generic classification of the Orthotrichaceae based on a molecular phylogeny and comparative morphology, pp 143–159. In: Bates JW, Ashton NW & Duckett JG (eds), Bryology for the Twenty-firstCentury. Maney Publishing and the British Bryological Society

Gradstein SR, Churchill SP, Salazar-Allen N (2001) Guide to the bryophytes of Tropical America. Mem N Y Bot Gard 86:1–577

Guo S-L, Ma Y-H, Cao T, Lou Y-X (2012) A synopsis of *Macromitrium* (Orthotrichaceae) in China. Cryptogam Bryol 33:341–355. https://doi.org/10.7872/cryb.v33.iss4.2012.341

Hebert PDN, Cywinska A, Ball SL, Dewaard JR (2003) Biological identifications through DNA barcodes. Proc R Soc b: Biol Sci 270:313–321. https://doi.org/10.1098/rspb.2002.2218

Hedenäs L (2009) Haplotype variation of relevance to global and European phylogeography of *Sarmentypnum exannulatum* (Bryophyta: Calliergonaceae). J Bryol 31:145–158

Hollingsworth PM, Graham SW, Little DP (2011) Choosing and using a plant DNA barcode. PLoS ONE 6:e19254. https://doi.org/10.1371/journal.pone.0019254

Kimura M (1980) A simple method for estimating evolutionary rate of base substitutions through comparative studies of nucleotide sequences. J Mol Evol 16:111–120. https://doi.org/10.1007/BF01731581

Kumar S, Stecher G, Tamura K (2015) MEGA7: molecular evolutionary genetics analysis version 7.0 for bigger datasets. Mol Biol Evol 33:1870–1974. https://doi.org/10.1093/molbev/msw054

Lang AS, Kruijer JD, Stech M (2014) DNA barcoding of Arctic bryophytes: an example from the moss genus *Dicranum* (Dicranaceae, Bryophyta). Polar Biol 37:1157–1169. https://doi.org/10.1007/s00300-014-1509-7

Larkin MA, Blackshields G, Brown NP, Chenna R, McGettigan PA, McWilliam H, Valentin F, Wallace IM, Wilm A, Lopez R, Thompson JD, Gibson TJ, Higgins DG (2007) Clustal W and Clustal X version 2.0. Bioinformatics 23:2947–2948. https://doi.org/10.1093/bioinformatics/btm404

Léon B, Rothfels CJ, Arakaki M, Young KR, Pryer KM (2013) Revealing a cryptic fern distribution through DNA sequencing: *Pityrogramma trifoliata* in the Western Andes of Peru. Am Fern J 103:40–48. https://doi.org/10.1640/0002-8444-103.1.40

Li DD, Guo S, Yu J (2013) Feasibility study on the identification of genus *Macromitrium* based on four chloroplast genes. Plant Sci J 31:23–33. https://doi.org/10.3724/SP.J.1142.2013.10023

Li DD, Guo SL, Fang YM (2019) Taxonomic notes on *Macromitrium catharinense* (Bryopsida) with its new synonyms. Nord J Bot 37:1–8. https://doi.org/10.1111/njb.02320

Liu Y, Yan HF, Cao T, Ge XJ (2010) Evaluation of ten plant barcodes in Bryophyta (Mosses). J Syst Evol 48:36–46. https://doi.org/10.1111/j.1759-6831.2009.00063.x

Medina R, Lara F, Goffinet B, Garilleti R, Mazimpaka V (2013) Unnoticed diversity within the disjunct moss *Orthotrichum tenellum* s.l. validated by morphological and molecular approaches. Taxon 62:1133–1152. https://doi.org/10.12705/626.15

Müller K (2005) SeqState—primer design and sequence statistics for phylogenetic DNA data sets. Appl Bioinform 4:65–69. https://doi.org/10.2165/00822942-200504010-00008

Müller K, Quandt D, Müller J, Neinhuis C (2006) PhyDE®: Phylogenetic Data Editor. www.phyde.de

Mullis KB, Faloona FA (1987) Specific synthesis of DNA in vitro via a polymerase-catalyzed chain reaction. Methods Enzymol 155:335–350. https://doi.org/10.1016/0076-6879(87)55023-6

Nagalingum NS, Schneider H, Pryer KM (2007) Molecular phylogenetic relationships and morphological evolution in the heterosporous fern genus *Marsilea*. Syst Bot 32:16–25. https://doi.org/10.1600/036364407780360256

Noguchi A (1967) Musci japonici VII. The genus *Macromitrium*. J Hattori Bot Lab 30:205–230

Pacak A, Szweykowska-Kulińska Z (2000) Molecular data concerning alloploid character and the origin of chloroplast and mitochondrial genomes in the liverwort species Pellia borealis. J Pl Biotechnol 2:101–108

Posada D (2008) jModeltest: phylogenetic model averaging. Mol Biol Evol 25:1253–1256. https://doi.org/10.1093/molbev/msn083

Pryer KM, Schuettpelz E, Huiet L, Grusz AL, Rothfels CJ, Avent T, Schwartz D, Windham MD (2010) DNA barcoding exposes a case of mistaken identity in the fern horticultural trade. Mol Ecol Res 10:970–985. https://doi.org/10.1111/j.1755-0998.2010.02858.x

Puillandre N, Lambert A, Brouillet S, Achaz G (2012) ABGD, automatic barcode gap discovery for primary species delimitation. Mol Ecol 21:1864–1877. https://doi.org/10.1111/j.1365-294X.2011.05239.x

Rambaut A, Drummond AJ (2013) Tracer v1.4. Available at http://beast.bio.ed.ac.uk/Tracer

Ronquist F, Teslenko M, Van Der Mark P, Ayres DL, Darling A, Ohna SH, Larget B, Liu L, Suchard MA, Huelsenbeck JP (2012) Mr. Bayes 3.2: efficient Bayesian phylogenetic inference and model choice across a large model space. Syst Biol 61:539–542. https://doi.org/10.1093/sysbio/sys029

Rooy JV, Wyk AEV (1992) A conspectus of the subfamily Macromitrioideae (Bryopsida: Orthotrichaceae) in Southern Africa. The Bryol 95:205–215. https://doi.org/10.2307/3243436

Saitou N, Nei M (1987) The neighbor-joining method: a new method for reconstructing evolutionary trees. Mol Biol Evol 4:406–425. https://doi.org/10.1093/oxfordjournals.molbev.a040454

Sharp AJ, Crum H, Eckel P (1994) The Mosses flora of Mexico. Mem N Y Bot Gard 69:1–1113

Shaw AJ (2000) Molecular phylogeography and cryptic speciation in the mosses, Mielichhoferia elongata and M. mielichhoferiana (Bryaceae). Mol Ecol 9:595–608

Shaw AJ, Cox CJ, Goffinet B, Buck WR, Boles SB (2003) Phylogenetic evidence of a rapid radiation of pleurocarpous mosses (Bryophyta). Evolution 57:2226–2241

Silvestro D, Michalak I (2012) raxmlGUI: a graphical front-end for RAxML. Org Divers Evol 12:335–337. https://doi.org/10.1007/s13127-011-0056-0

Simmons MP, Ochoterena H (2000) Gaps as characters in sequence based phylogenetic analyses. Syst Biol 49:369–381. https://doi.org/10.1093/sysbio/49.2.369

Stech M, Frahm J-P (1999) Systematics of species of Eurhynchium, Rhychostegiella and Rhynchostegium (Brachytheciaceae, Bryopsida) based on molecular data. Bryobrothera 5:203–211

Stech M, Frey W, Frahm JP (1999) The status and systematic position of Hypnobartlettia fontana Ochyra and the Hypnobartlettiaceae based on molecular data. Studies in austral temperate rain forest bryophytes 4. Lindbergia 24:97–102.

Swofford DL (2002) PAUP* phylogenetic analyses using parsimony (*and other methods), version 4.0. Sinauer Associates, Sunderland, Massachusetts

Thouvenot L (2019) A review of the genus *Macromitrium* Brid. (Orthotrichaceae, Bryophyta) in New Caledonia. Cryptogam Bryol 40:167–217. https://doi.org/10.5252/cryptogamie-bryologie2019v40a16

Valente DV, Câmara PEAS, Peralta DF, Stech M (2019) Molecular tools to identify tropical mosses: a case study of the Brazilian species of *Schlotheimia* Brid. (Bryophyta, Orthotrichaceae). Syst Biodivers 17:609–621. https://doi.org/10.1080/14772000.2019.1655110

Vitt DH, Ramsay HP (1983) The New Zealand species of the pantropical moss *Macromitrium* (Orthotrichaceae: Musci) taxonomy, phylogeny and phytogeography. J Hattori Bot Lab 54:1–94

Vitt DH, Ramsay HP (1985a) The *Macromitrium complex* in Australasia (Orthotrichaceae, Bryopsida). Part I. Taxonomy and phylogenetic relationships. J Hattori Bot Lab 59:325–451

Vitt DH, Ramsay HP (1985b) The *Macromitrium* complex in Australasia (Orthotrichaceae, Bryopsida). Part II. Distribution, ecology, and paleogeography. J Hattori Bot Lab 59:453–468

Vitt DH, Ramsay HP (1986) The *Macromitrium* complex in Australasia (Orthotrichaceae: Bryopsida). Part III. Cytotaxonomy. J Hattori Bot Lab 61:1–43

Vitt DH (1990) *Desmotheca* (Orthotrichaceae): Gondwanan fragmentation and the origin of a Southeast Asian genus. Trop Bryol 3:79–88. https://doi.org/10.11646/bde.3.1.10

Vitt DH, Koponen T, Norris DH (1995) Bryophyte flora of the Huon Peninsula, Papua New Guinea. LV. *Desmotheca, Groutiella, Macrocoma* and *Macromitrium* (Orthotrichaceae, Musci). Acta Bot Fenn 154:1–194

Wilbraham J (2015) Annotated checklist and keys to the Orthotrichaceae of Malawi, together with new country records for East Africa. J Bryol 37:1–10. https://doi.org/10.1179/1743282014Y.0000000133

Wilbraham J (2016) Taxonomic notes on African Orthotrichaceae I. New synonymy in *Macromitrium*. J Bryol 38:87–93. https://doi.org/10.1080/03736687.2015.1124175

Yu J, Guo S-L, Lou Y (2018) Three new synonyms of *Macromitrium microstomum* (Hook. & Grev.) Schwägr. (Bryophyta, Orthotrichaceae), with comments on its morphological variations. J Bryol 40:1–9. https://doi.org/10.1080/03736687.2018.1484679